CHALMERS
UNIVERSITY OF TECHNOLOGY

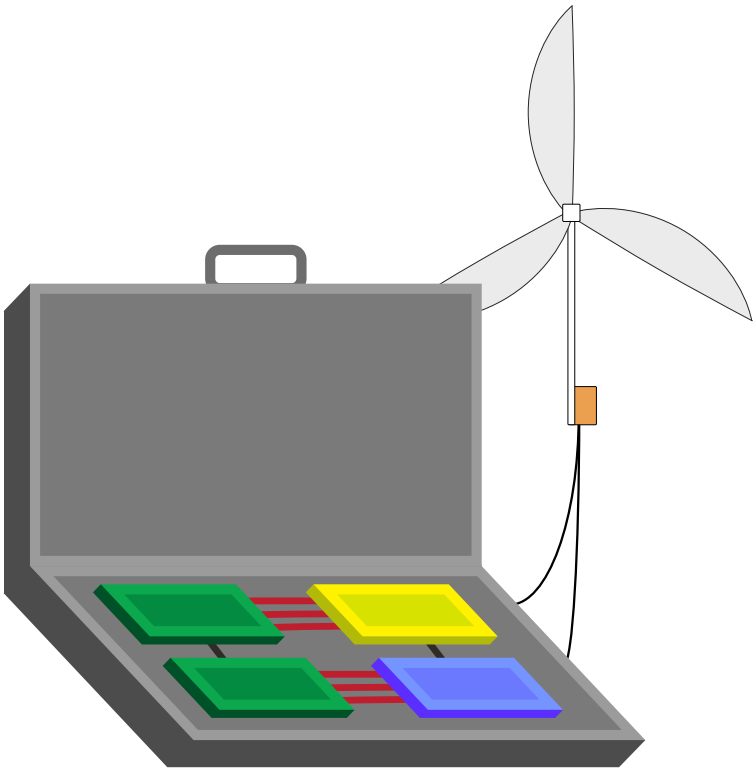

Enhancing Grid Stability through Advanced Power Plant Performance Testing

Design and Development of Inverter-Based Testing Equipment for Comprehensive Power Plant Performance Assessment

Master's thesis in Sustainable Electric Power Engineering and Electromobility

David Emanuelsson
Jesper Nilsson

DEPARTMENT OF ELECTRICAL ENGINEERING
CHALMERS UNIVERSITY OF TECHNOLOGY
Gothenburg, Sweden 2024
www.chalmers.se

Master's thesis 2024

Enhancing Grid Stability through Advanced Power Plant Performance Testing

Design and Development of Inverter-Based Testing Equipment for Comprehensive Power Plant Performance Assessment

David Emanuelsson
Jesper Nilsson

CHALMERS
UNIVERSITY OF TECHNOLOGY

Department of Electrical Engineering
Division of Electric Power Engineering
Chalmers University of Technology
Gothenburg, Sweden 2024

Enhancing Grid Stability through Advanced Power Plant Performance Testing
Design and Development of Inverter-Based Testing Equipment for Comprehensive Power Plant Performance Assessment
David Emanuelsson, Jesper Nilsson

Supervisor: Andreas Petersson, Protrol Engineering AB
Examiner: Massimo Bongiorno, Department of Electrical Engineering, Chalmers

Master's Thesis 2024
Department of Electrical Engineering
Division of Electric Power Engineering
Chalmers University of Technology
SE-412 96 Gothenburg
Telephone +46 31 772 1000

Typeset in LaTeX
Printed by Chalmers Reproservice
Gothenburg, Sweden 2024

Enhancing Grid Stability through Advanced Power Plant Performance Testing
Design and Development of Inverter-Based Testing Equipment for Comprehensive Power Plant Performance Assessment
David Emanuelsson & Jesper Nilsson
Department of Electrical Engineering
Chalmers University of Technology

Abstract

In the shift to renewable energy sources, traditional electricity production is disrupted, posing new demands to maintain grid stability. Regulations regarding increased requirements for frequency regulation have therefore been adopted in Europe. To ensure compliance with these regulations, extensive testing of power generation facilities is needed.

The project has contributed to further development of testing equipment aimed at testing power plant performance in regulating its output power given frequency deviations in the power system. Power plants are fed back from the power system via transducers to be able to control appropriate output signal. In power plants, there are various types of transducers for the conversion of various electrical quantities. Modern transducers can transmit all electrical quantities, so-called multi-transducers. The project's goal has been to make the existing testing equipment compatible with all the quantities that the power plant transducers can provide. To enable compatibility with voltage and current, two inverter with a mutual control unit have been designed. The test equipment replaces the feedback loop from the power generating system and creates artificial test signals to evaluate the power plant's response to various changes in the power system. The testing equipment's signals imitate the characteristics of the power system in terms of voltage and current with corresponding phase shifts in three phases.

In addition, a study of what impact the transducer itself has on the closed loop system has been conducted. The study has been carried out in the simulation program Simulink, where the transducer has been modelled as either a time delay or a low-pass filter, as well as the combination of the two, in models of hydropower plants and battery storage.

Simulated results show good performance in terms of accuracy and response to setting changes. Construction of a physical prototype has begun, where the inverter controlling the product's voltage has shown promising results. The inverter intended to control the product's current output requires further work. The study concerning the performance of the transducer shows little or no impact on the two models.

Keywords: RfG, PWM-technology, PSCAD, Power electronics, Power systems, Inverter, Test equipment, Control, Simulink, Matlab.

Enhancing Grid Stability through Advanced Power Plant Performance Testing
Design and Development of Inverter-Based Testing Equipment for Comprehensive Power Plant Performance Assessment
David Emanuelsson & Jesper Nilsson
Department of Electrical Engineering
Chalmers University of Technology

Sammanfattning

I skiftet till förnyelsebara energikällor rubbas den traditionella elektricitetsproduktionen vilket ställer nya krav för att bibehålla elnätets stabilitet. Föreskrifter som avser ökade krav på frekvensreglering har därför antagits i Europa. För att garantera att dessa föreskrifter uppfylls, behövs omfattande testning av kraftproduktionsanläggningar.

Projektet har bidragit till vidareutveckling av en testutrustning med syfte att testa kraftverks prestanda att reglera sin uteffekt givet frekvensavvikelser i kraftsystemet. Kraftverk återkopplas med kraftsystemet via mätvärdesomvandlare för att kunna styra lämplig utsignal. I kraftverk finns olika modeller av mätvärdesomvandlare för omvandling av olika elektriska storheter. Moderna mätvärdesomvandlare kan överföra samtliga elektriska storheter, så kallade multiomvandlare. Projektets mål har varit att göra den existerande testutrustningen kompatibel med alla storheter som kraftverkens mätvärdesomvandlare kan tillhandahålla. För att möjliggöra kompabilitet med spänning och ström har två omriktare med gemensam styrenhet designats. Testutrustningen ersätter återkopplingen från kraftsystemet och skapar konstgjorda testsignaler för att kunna utvärdera kraftverkets respons på olika avvikelser i kraftsystemet. Testutrustningens signaler imiterar kraftsystemets karaktäristik i form av spänning och ström med tillhörande fasförskjutning i tre faser.

Dessutom har en studie av mätvärdesomvandlarnas påverkan på det återkopplade systemet genomförts. Studien har utförts i simuleringsprogrammet Simulink, där mätvärdesomvandlaren har modellerats som antingen en tidsfördröjning eller ett lågpassfilter, samt kombinationen av de två, i modeller av vattenkraftverk och batterilager.

Simulerade resultat visar på god prestanda med avseende på noggrannhet samt respons på ändringar i inställningar. Ett bygge av fysisk prototyp har påbörjats, där omriktaren som styr produktens spänning visat goda resultat. Inverteraren som skall styra produktens strömutsignal kräver ytterligare arbete. Studien som avser att utvärdera mätvärdesomvandlarnas prestanda har påvisat liten eller ingen påverkan på vattenkraftsmodeller och batterilagersmodeller.

Keywords: RfG, PWM-teknik, PSCAD, Kraftelektronik, Kraftsystem, Inverterare, Testutrustning, Kontroll, Simulink, Matlab.

Acknowledgements

We would like to express our sincere gratitude to all of those who have contributed to the completion of this thesis. First and foremost, we want to thank our supervisor, Andreas Petersson, for his invaluable guidance, support, and encouragement throughout this thesis work. We would also like to express our gratitude to the employees at Protrol Engineering AB for their support and offering of a welcoming workplace.

David Emanuelsson and Jesper Nilsson, Gothenburg, June 2024

List of Acronyms

Below is the list of acronyms that have been used throughout this thesis listed in alphabetical order:

AC	Alternating Current
ADC	Analog to Digital Converter
CSI	Current Source Inverter
DC	Direct Current
DT	Duty Time
EU	European Union
FFT	Fast Fourier Transform
IGBT	Insulated-Gate Bipolar Transistor
MPU	Microprocessor Unit
PWM	Pulse Width Modulation
RFG	Requirements for Generators
RMS	Root Mean Square
SVK	Svenska Kraftnät
TSO	Transmission System Operator
VSI	Voltage Source Inverter

Contents

List of Figures

List of Tables

1
Introduction

The growing demand for power in today's power systems underscores the critical need for reliability, ensuring operation without the risk of failure. Regular testing of system components becomes necessary to uphold this reliability. This necessity is further strengthened as the energy landscape evolves with an increased share of renewable sources, which generally lacks inertia. Due to decreased system inertia, the power system becomes more susceptible to frequency deviations. Generators to be connected to the power system need to be tested so that its connection does not worsen the system stability.

To ensure that electricity is delivered with high quality, a robust power system network is needed. A crucial point of the power system is the generators which undergo rigorous testing to ascertain their capability to provide ancillary services to the system when required. These services encompass critical functions such as frequency regulation, aimed at stabilizing the system frequency in the event of deviations from the reference frequency.

Frequency containment reserve (FCR), a vital component of ancillary services, is crucial for maintaining system stability. It is subdivided into two categories based on operational requirements:

- **FCR-N (Normal Drift):** Activated within the frequency range of 49.9-50.1 Hz, FCR-N ensures steady frequency control, minimizing deviations from the fundamental 50 Hz frequency during normal system operation.
- **FCR-D (Drastic Drift):** Triggered when frequency deviations exceed normal operational parameters, FCR-D facilitates corrective actions to bring the system back to equilibrium. FCR-D further divides into two operations:
  - **FCR-D Up Regulation:** Engaged when the frequency drops below 49.90Hz, necessitating an increase in frequency to restore stability.
  - **FCR-D Down Regulation:** Activated when the frequency exceeds 50.10Hz, requiring a reduction in frequency to mitigate overloading and maintain system balance.

Effective testing and implementation of ancillary services like FCR are essential for ensuring the resilience and reliability of the power system network [1].

In summary, generators need to be tested for several purposes. The tests include compliance tests such as voltage and frequency control, fault ride through and dynamic performance. Additionally, generators need to be tested for their ability to provide ancillary services. Through rigorous testing, generators can be verified to meet the necessary

criteria for the RfG legislation and for providing ancillary services.

1.1 Background

In power plants, there are speed governors that regulates the injected fuel corresponding to the load of the grid. The speed governor ensures that the turbine rotates in optimal speed to maintain the frequency of the electrical power generated. As the power demand fluctuates in the grid, the speed governor adjust the turbine speed and power output. When the load on the grid increases, the speed governor increases fuel supply to the turbine to maintain the frequency of the grid.

Protrol Engineering AB (Protrol) currently employ tests in power production facilities with a self-designed test equipment called HzOn. Normally, the speed governor of the power production facility is continuously taking data from the grid to regulate the output of the facility. When using HzOn, the speed governor is instead fed by HzOn's test signals, see Fig. 1.1. The signals are voltage signals with controllable frequency. The frequency can be varied to study the response of the facility at different frequency deviations.

In power production facilities, different types of transducers are available. Modern transducers can extract multiple electrical quantities such as frequency and active- and reactive power. Currently, HzOn is solely compatible with frequency transducers. To obtain the frequency, a voltage signal is enough. However, if the transducer feed the regulator with active or reactive power, the current is required as well. To use HzOn with power compatible transducers, an expansion to current manageability is required.

The improved testing equipment must possess the capability to execute a range of tasks, including verifying the adequacy and accuracy of support from ancillary services to ensure seamless system performance. Additionally, it should assess the system's capacity to function autonomously in islanded operation scenarios. Furthermore, the equipment must facilitate grid measurements and exercise control over the protection mechanisms of power production facilities. It should also verify whether the relays would activate in accordance with predefined settings in the event of a fault occurrence.

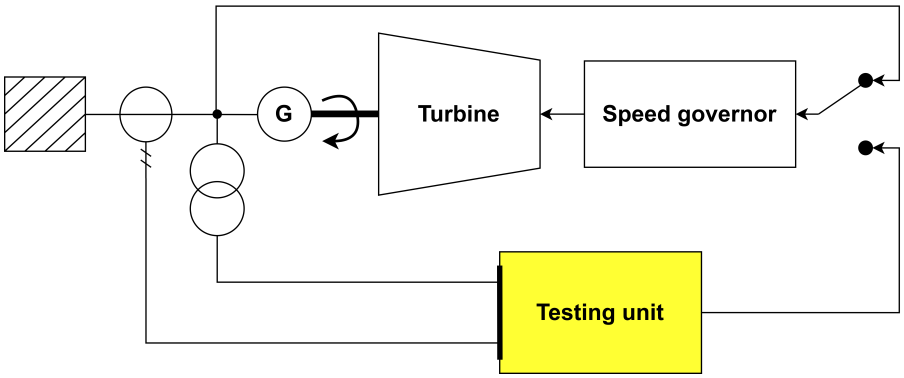

Figure 1.1: The current testing unit (HzOn) provides the speed governor with simulated frequency signals and the response is measured to evaluate the performance and reliability of the power production facility.

In order to create a portable and compact device that can fit within a suitcase, two converters based on PWM technique are to be designed. The two converters are to be synchronized, controlled from a single control unit. One Current regulating Voltage Source Inverter (VSI) and one voltage regulating VSI. The desired output is to be controllable from an interface. The work can be divided into simulation, implementation, and evaluation. Simulations of the C-based programmed controller will be performed controlling a half-bridge in PSCAD. Further, the PWM-controller will be implemented on a microprocessor unit (MPU) controlling a physical half bridge circuit. The system will be evaluated based on its accuracy and response to changes in input.

The improved HzOn will be able to obtain the desired active power, reactive power, voltage level and frequency by regulating the corresponding current to the set output voltage, see Fig. 1.2.

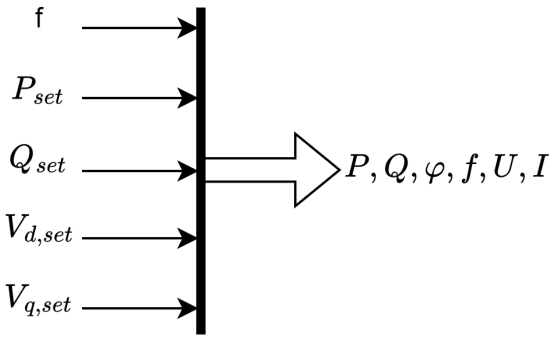

Figure 1.2: The system is to be able to create test signals with the desired characteristics based on user inputs.

1.1.1 Aim

The aim of this master thesis project is to design a control system for mutual regulation of a current regulating VSI and a voltage regulating VSI based on sinusoidal PWM-

technique. The system is to be able to provide the correct voltage and current with corresponding phase angle to ensure the correct active and reactive power.

1.1.2 Specification of the Issue Being Investigated

New and/or modernized production facilities have nowadays transducers providing both voltage and current, compared to the older transducers that only provided voltage. The problem in focus is to further develop an existing testing unit that can only take voltage signal, to be able to handle both a voltage and current signal as input.

The project is divided into the following parts:

- Simulate the performance of a current regulating VSI and a voltage regulating VSI in PSCAD.
- Evaluate the effect of transducer's inherent properties on the control system's performance and stability.
- Program a microprocessor with the instructions of the controller in the PSCAD model.
- Perform hardware test on existing half-bridge circuit with the programmed microprocessor.

1.1.3 Limitations

This project's purpose is to develop the control system of already existing hardware. This project will therefore not include any hardware design or further investigation of alternative hardware circuits. Neither the DC-voltage nor the current source will be considered but be handled as a variable input in the model simulations.

The project is based on an older project and will not involve any change in the current design, only the added parts will be evaluated.

1.1.4 Ethical Considerations

The IEEE Code of Ethics is a set of principles and guidelines that members of the IEEE are encouraged to follow in their professional activities [2]. In order to maintain a certain order of responsible behavior in this paper and project, the authors strive to work by these principles. The IEEE Code of Ethics consists of ten principles, where some are more applicable to this paper. Here follows some of the principles and how the authors are to relate to them:

1. "to hold paramount the safety, health, and welfare of the public, to strive to comply with ethical design and sustainable development practices, to protect the privacy of others, and to disclose promptly factors that might endanger the public or the environment;"[2]

This principle underscores the importance of ensuring that the control system design prioritizes safety and avoids any risks to the users or the environment.

5. "to seek, accept, and offer honest criticism of technical work, to acknowledge and correct errors, to be honest and realistic in stating claims or estimates based on

available data, and to credit properly the contributions of others;" [2]

This principle emphasizes the importance of constructive criticism, acknowledging mistakes, and giving credit to contributors. Protrol are to support the authors with knowledge in the area of subject. Further, Chalmers University of Technology are to give feedback of the project. In a project involving complex systems like a control system, open communication and learning from feedback are critical. Since this master thesis project includes designing test equipment used to test vital points of operation, being critical to the results and acknowledging mistakes is crucial.

1.1.4.1 Ecological Aspects

Implementing new and enhanced testing procedures for power production units can significantly contribute to establishing a more robust and stable grid network. With a consistent and reliable influx of power from production units, the system would experience reduced reliance on short-term measures, such as burning fossil fuels, to meet immediate power demands. Enhanced reliability in renewable power generation would consequently diminish the necessity for fossil fuel-based production methods.

Sweden has relatively low carbon footprint in energy generation, largely attributed to its extensive utilization of renewable energy sources. However, during instances when Sweden cannot meet its power generation requirements, it resorts to importing electricity from neighboring countries. Many of these countries rely heavily on power generation from fossil fuels to fulfill their energy needs.

Reducing the dependency on imports would be advantageous for Sweden in maintaining its low carbon footprint in power generation. Therefore, strengthening the reliability of domestic power production through improved testing procedures holds the potential to positively impact Sweden's environmental sustainability goals.

1.1.4.2 Social Aspects

In the approach of social aspects, reliable power production units in the electric grid could ease the minds of its users. When a fault occurs somewhere in the grid, people will be less bothered since it has small impact on people's everyday life. Also, vital points of operations who are primary functions in preparedness in Sweden like healthcare and communication usually have the possibility to support oneself in island operation in case of emergency [3]. Accurate and reliable tests is essential to rely on those functions.

1.1.4.3 Economical Aspects

In an economical point of view, it is cheaper for countries to generate its own electricity, especially if that source of generation is from a renewable source. Current trends show that generation from renewable sources is becoming cheaper. It is important to have renewable sources of generation operational at all times to avoid having to import electric power from other countries. To have generation operational at all times, regular testing is beneficial to the system [4].

2
Theory

2.1 Generator Testing Setup

For testing of power generating facilities the system consists of the generator, turbine, speed governor with the testing unit coupled as feedback. The system can look different depending on the factors like what type of power generating facility it is and what type of transducer the facility is fitted with. For some power facilities there exists transducers that only needs a voltage input to be able to measure the frequency. There also exists newer transducers which have both voltage and current input, where both the frequency but also the power can be regulated to test the generators. To test the system then according to testing protocols from SVK then the feedback loop from the system is disconnected and instead a digital signal which is then translated to an analog signal is pushed through instead. The signal contains different scenarios for how the grid could act and to see if the generator does appropriate actions to promote the grid stability. Generators are tested for if they give out an appropriate amount of support in case the system have changes in the frequency.

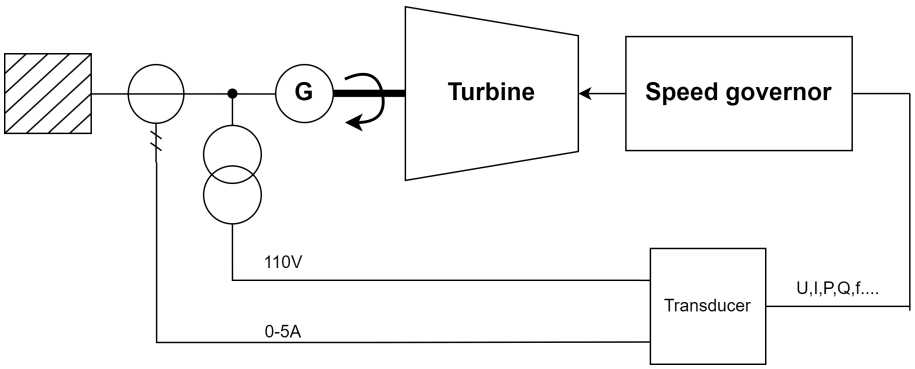

Figure 2.1: Generator default setup.

During normal operation the generator output is determined by the measured values from the transducer. The setup for when the generator functions normally is seen in Fig. 2.1. The transducer will take in values from the grid which are then transformed to suit the transducer which then the transducer will convert into digital control signal telling the generator how to operate. From the transducer then different quantities can get extracted like the voltage, current, active power, reactive power and frequency but these are the only ones utilized while the transducer can emit more types.

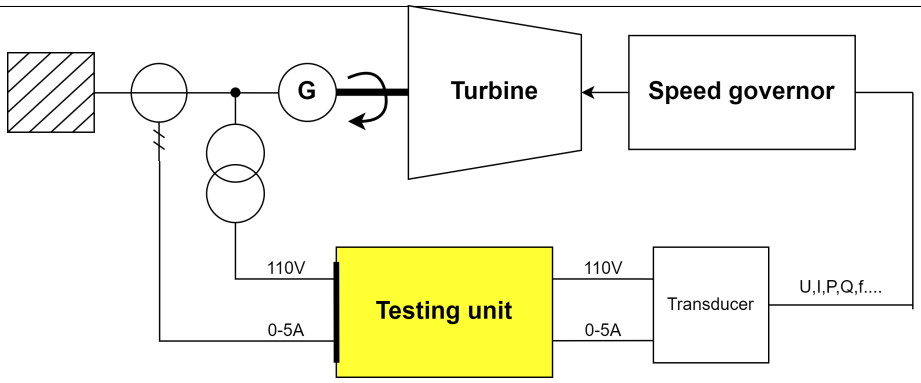

Figure 2.2: Generator setup during testing.

Here Fig. 2.2 shows how the test equipment is set up during testing. The signals come from the testing unit into the transducer instead of coming from the grid, then values of the units can instead be given from the testing operator. The testing operator can then input their own values to create different scenarios for the generator and then measurements can be taken on the generator to see if appropriate amount of regulatory action is taken.

2.2 Inverter Management Using Sinusoidal PWM

When designing control of power electronics, it is important to understand the dynamics of the system to anticipate the system behavior. Also, when designing a control system, it is important to respect the limitations of the hardware. The limitations due to the hardware usually requires some compensation in the control design, and what the best solution is depends on the product's application.

2.2.1 Controller Design

The design of controllers for electrical circuits is a critical aspect to ensure efficient and stable operation. One common scenario in the control of current is in resistance-inductance-circuits (RL-circuits), see Fig. 2.3. The objective of the controller is to regulate the current flowing through the load and minimizing the deviations from the reference value. It is therefore important to understand characteristics of the load. The behavior of RL-circuits is characterized by its time delays and dynamic response. RL-circuits can be seen as a first order low pass filter according to Equation (2.5), derived from Equations (2.1)-(2.3). The input voltage u(t) in Fig. 2.3 can be expressed as

$$u(t) = Ri(t) + L\frac{di(t)}{dt} \tag{2.1}$$

Where L$\frac{di(t)}{dt}$ is the voltage over the inductance and Ri(t) is the voltage over the resistance in the RL-circuit. Laplace transform of Equation (2.1) gives

$$U(s) = RI(s) + LsI(s) \tag{2.2}$$

where

$$Y(s) = RI(s) \tag{2.3}$$

and

$$I(s) = \frac{U(s)}{R + Ls} \tag{2.4}$$

Combining Equation (2.2)-(2.3) with Equation (2.4) gives the transfer function H(s)

$$H(s) = \frac{Y(s)}{U(s)} = \frac{R}{R + Ls} = \frac{\frac{R}{L}}{\frac{R}{L} + s} = \frac{\alpha}{\alpha + s} \tag{2.5}$$

Where α = R/L and represents the cutoff frequency of the lowpass filter.

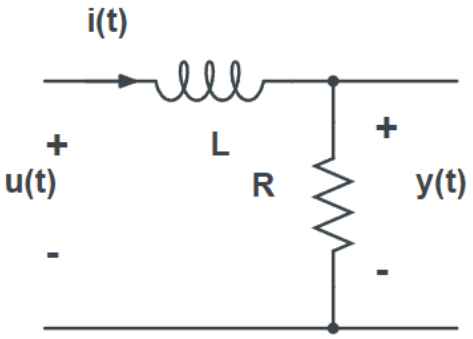

Figure 2.3: RL-circuit.

Block diagrams can be used to visualize the design process of control systems. Fig. 2.4 depicts a block diagram of a closed-loop current control system, where e represents the error (difference between i_{ref} and i), F(s) the controller, D the disturbance to be compensated for and G(s) the dynamics of the load.

Proportional-Integral (PI) controllers are commonly used in current control systems. The proportional part of the PI-controller responds to the current error instantaneously while the integral part eliminates the steady state error over time. The proportional gain K_p and integral gain K_i need to be carefully tuned for optimal performance. The gains of the controller need to be tuned to achieve acceptable response time while maintaining system stability and robustness.

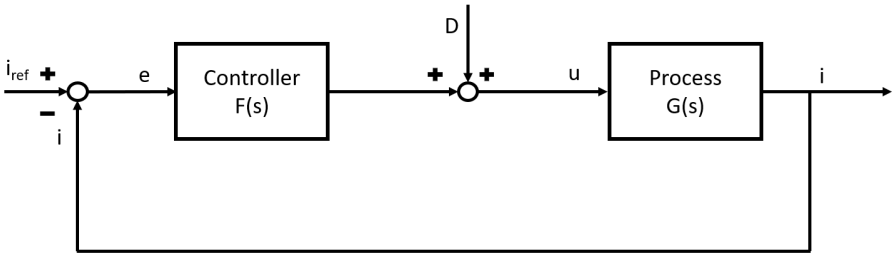

Figure 2.4: Block scheme of a closed-loop system.

2.2.2 STM32 Programming

STM32 is a group of 32-bit microcontroller units by STMicroelectronics. To program the STM cards a software called STM32CubeIDE can be used. STM32CubeIDE is a C/C++ development environment with many pre-built functions which can be enabled easily through their interface.

STM32 microcontrollers are suitable for PWM control and many of them come with PWM-related pre-defined functions that ease their manageability. Building PWM controlled inverters require PWM signals to control the inverter's switches. To generate the PWM signals in STM32CubeIDE, built in timers need to be configured. There are usually several timers on each microprocessor. The timers are divided into Advanced Timers and General Purpose Timers. The advanced timers have more channels for PWM output, more advanced trigger and synchronization capabilities, and higher resolution. The advanced timers is therefore useful when three phase PWM generation is required.

In the STM32F407G-DISC1 used in this project, there are two advanced timers in which each one of them is used to send out PWM control signals to each of the two inverter circuits.

2.2.3 Effect of Blanking Time in PWM Inverters

In the discussion about PWM, the switches normally are assumed to be ideal. However, in reality, to avoid shoot-through in the inverter legs the turn on and off of the switches of the inverter leg is delayed by a blanking time. The blanking time can affect shape, amplitude and introduce distortions to the output signal and is therefore important to consider and it is in some applications necessary to compensate for the blanking time.

Since both switches are off during the blanking time t_Δ, the phase voltage v_{AN} depends on the direction of the phase current i_A, see Fig. 2.5. By averaging the difference between the ideal output voltage and the actual output voltage, the change in output voltage ΔV can be obtained [5]:

$$\Delta V = \begin{cases} +\frac{t_\Delta}{T_s} V_d & \text{if } i_A > 0 \\ \\ -\frac{t_\Delta}{T_s} V_d & \text{if } i_A < 0 \end{cases} \tag{2.6}$$

where V_d is the DC-voltage feeding the inverter and,

$$T_s = \frac{1}{f_s} \tag{2.7}$$

where f_s is the switching frequency. This implies that ΔV is proportional to the blanking time t_Δ and the switching frequency f_s. In high frequency applications fast switching devices such as MOSFETs and IGBTs enabling small t_Δ should be used in order to minimize the change in output voltage ΔV.

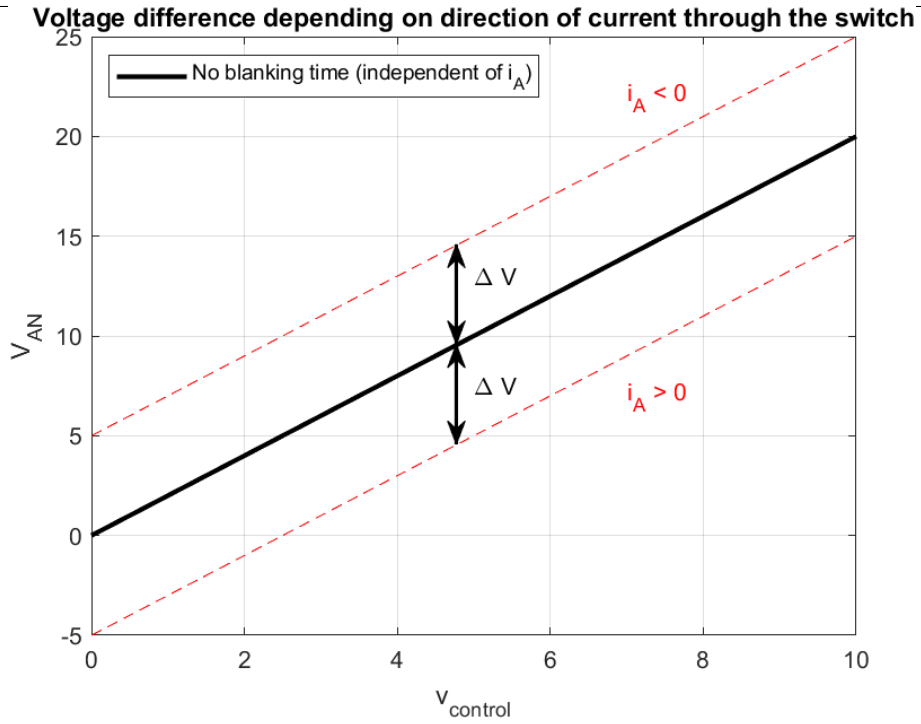

Figure 2.5: Effect of blanking time on the output voltage based on the direction of the current.

The distortion in output voltage at the current zero crossing results in harmonics in the phase-to-phase voltages of the three-phase inverter. The order of harmonics are $6m \pm 1$ (m=1,2,3,...) of the fundamental frequency [5].

2.2.4 Switching Frequencies

Switching frequency in terms of PWM inverter is at what frequency the switches in the inverter bridge switch on and off. High switching frequency allow for fine control of the output voltage waveform and fast regulation. Electromagnetic interference (EMI) and switching losses typically increase with the frequency. High frequency distortions is however easy to attenuate using filter.

In STM32CubeIDE it is possible to adjust the switching frequency and the frequency at which the duty time of the PWM signals is recalculated. Throughout this project, the switching frequency used is 10kHz. This frequency allows fast regulation and distortions at high frequency compared to the fundamental frequency at 50Hz, enabling efficient filtering.

3
Methods

The objective of the project is to create a microprocessor-based control board regulating output of two separate inverters to achieve desired power and frequency. To describe the approach, the Method chapter is divided into Regulating Systems 3.1 describing the code running in the microprocessor to regulate the output signals to have desired characteristics, Filter Design 3.2 describing the procedure of designing suitable filters, and lastly Working Connections 3.3-3.4 describing the circuits of respective inverter.

3.1 Control Systems

To obtain the desired active power P and reactive power Q at desired frequency f, a feedback PI-regulator was introduced at the current providing inverter. The current is regulated to provide the correct phase shift and magnitude corresponding to the desired power. To simplify the control procedure, the setpoint values of the current and voltage are set in dq-coordinates. The voltage is regulated in open loop as $V_d = 110\ V_{rms}$ and $V_q = 0\ V_{rms}$. The current is closed loop regulated and the setpoint values of the current is calculated from the desired power (assuming $V_q = 0$) as

$$I_{d,set} = \frac{P}{V_{d,set} \cdot \frac{\sqrt{3}}{\sqrt{2}}} \tag{3.1}$$

and

$$I_{q,set} = \frac{-Q}{V_{d,set} \cdot \frac{\sqrt{3}}{\sqrt{2}}} \tag{3.2}$$

, where $V_{d,set}$ is the constant phase-to-phase rms setpoint value of the voltage in the voltage regulated converter. The measured current is transformed into dq-coordinates before the error between the setpoint values and the measured values are calculated in the regulator. The method employed by the system is thoroughly elaborated upon in the following subsections.

3.1.1 Synchronous Coordinates

In three-phase circuits, transformation to synchronous coordinates, also called the DQ-coordinates, is a mathematical technique used to simplify the analysis and control of the three-phase systems. The DQ-reference frame rotates synchronized with the electrical angular position. The transformation to the DQ-reference frame is used to remove the rotation of the vectors representing the AC waveforms, thereby converting them into DC

signals. Simplified analysis and implementation of control algorithms can then be carried out before performing the inverse transformation to recover the actual three-phase results.

The transformation to DQ-coordinates consists of the Clarke and Park transform. The Clarke transform converts vectors in the ABC-reference frame to the $\alpha\beta$-reference frame given by:

$$\begin{bmatrix} V_\alpha \\ V_\beta \end{bmatrix} = K \begin{bmatrix} \frac{2}{3} & -\frac{1}{3} & -\frac{1}{3} \\ 0 & \frac{1}{\sqrt{3}} & -\frac{1}{\sqrt{3}} \end{bmatrix} \begin{bmatrix} V_a \\ V_b \\ V_c \end{bmatrix} \tag{3.3}$$

Where V_a, V_b, and V_c are the phase voltages and V_α and V_β are the α-axis and β-axis components of the voltage in the stationary reference frame. The scaling factor K can be arbitrarily chosen based on the specific application. For instance, setting $K = 1$ yields the peak voltage, while $K = \frac{1}{\sqrt{2}}$ corresponds to the rms-value. Alternatively, selecting $K = \sqrt{\frac{3}{2}}$ yields the power invariance. The scaling factor K for peak voltage is used throughout this project.

Further, the Park transform converts vectors in the $\alpha\beta$-reference frame to the DQ-reference frame given by:

$$\begin{bmatrix} V_d \\ V_q \end{bmatrix} = \begin{bmatrix} \cos(\theta) & \sin(\theta) \\ -\sin(\theta) & \cos(\theta) \end{bmatrix} \begin{bmatrix} V_\alpha \\ V_\beta \end{bmatrix} \tag{3.4}$$

Where V_d and V_q are the d-axis and q-axis components of the voltage in the synchronous reference frame and θ is the electrical angle obtained by integrating the angular velocity as

$$\int f(t) \cdot 2\pi \, dt = \theta(t) + C. \tag{3.5}$$

In Fig. 3.1 the block implementation of the electrical angle θ tracking is depicted.

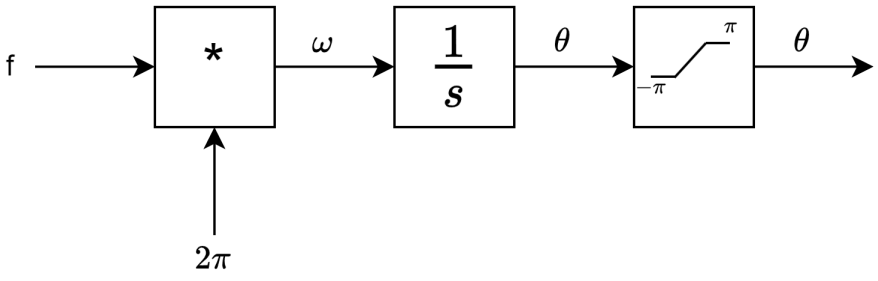

Figure 3.1: Simple block implementation of the electrical angle tracking.

The conceptual implementation of the current regulation including frame transformations can be seen in Fig. 3.2.

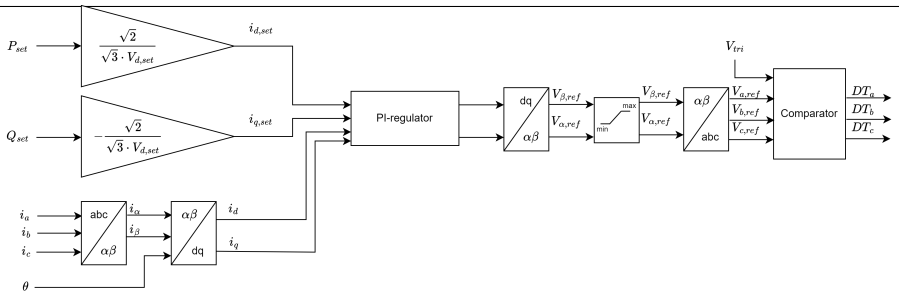

Figure 3.2: Conceptual implementation of the current regulation calculating the duty times (DT) based on the desired active power P_{set} and reactive power Q_{set} and the measured phase currents (i_a, i_b, i_c).

The voltage regulation is open loop, thus the conceptual implementation seen in Fig. 3.3 is simpler than the closed loop current regulating system.

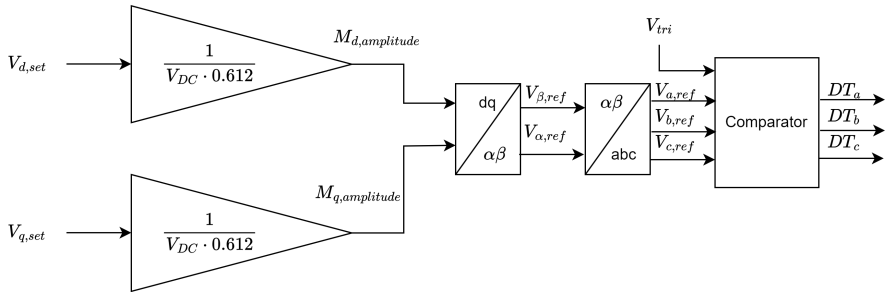

Figure 3.3: Conceptual implementation of the voltage regulation calculating the duty times (DT) based on the desired voltage levels.

3.1.2 Compensation in DQ

The voltage U in a RL-circuit can be expressed as

$$U = Ri + L\frac{di}{dt}. \tag{3.6}$$

In DQ coordinates this corresponds to

$$U = R\underline{\mathbf{i}} + L\frac{d\underline{\mathbf{i}}}{dt} + j\omega L\underline{\mathbf{i}}. \tag{3.7}$$

where

$$\underline{\mathbf{i}} = i_d + ji_q. \tag{3.8}$$

The introduced $j\omega L$ component is related to the rotating frame when transforming into the DQ-coordinates. Let us substitute $\underline{\mathbf{u}}^* = R\underline{\mathbf{i}} + L\frac{d\underline{\mathbf{i}}}{dt} = u_d^* + u_q^*$, then

$$U = \underline{\mathbf{u}}^* + j\omega L i_d - \omega L i_q. \tag{3.9}$$

If the voltage components U_d and U_q are regulated to be

$$U_d = u_d^* - \omega L i_q \tag{3.10}$$

$$U_q = u_q^* + j\omega L i_d \tag{3.11}$$

and

$$U_q + U_d = u_q^* + j\omega L i_d + u_d^* - \omega L i_q = \underline{\mathbf{u}}^* + j\omega L i_d - \omega L i_q \tag{3.12}$$

then the ωL-components are cancelled out, meaning that u_d^* and u_q^* is the output voltage in respective coordinate.

$$U = U_d + U_q$$
$$\underline{\mathbf{u}}^* + \cancel{j\omega L i_d} - \cancel{\omega L i_q} = \underline{\mathbf{u}}^* + \cancel{j\omega L i_d} - \cancel{\omega L i_q}$$

The PI-regulator is depicted in Fig. 3.4.

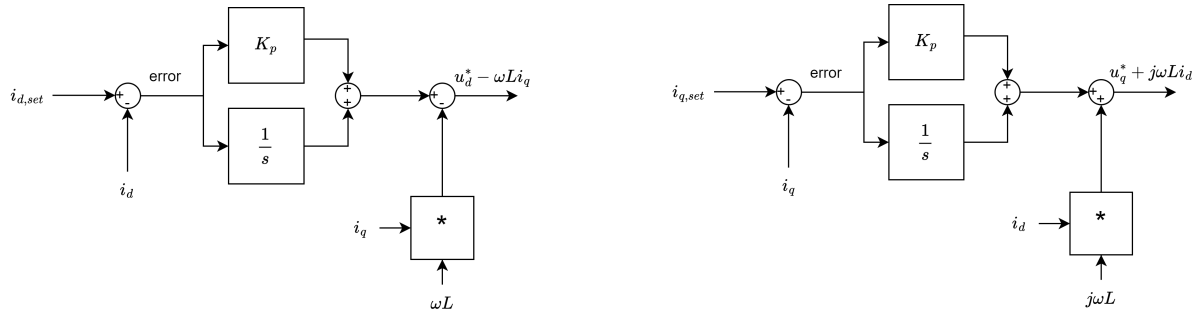

(a) PI-regulator for the d-component current.

(b) PI-regulator for the q-component current.

Figure 3.4: The PI-regulator compensates for the ωL-components in DQ-frame.

3.1.3 PI-Controller Parameter Calculations

Since the system parameters are well known or estimated as described in Section 2.2.1, suitable proportional gain K_p and integral gain K_i of the PI-controller can be calculated. Initially, the requirement of the system, such as rise time t_{re}, needs to be specified. The rise time is set to be in the millisecond range. The transfer function G_{cl} of the closed loop system depicted in Fig. 3.5 can be represented as a low pass filter [6] according to

$$G_{cl} = \frac{\alpha_c}{\alpha_c + s} = \frac{1}{sT_e + 1}, \quad \alpha_c = \frac{1}{T_e}[7]. \tag{3.13}$$

Where α_c is defined as the closed loop system bandwidth and T_e is the electrical time constant (0-63%). The relationship between the rise time t_{re} (10-90%) and the time constant T_e is

$$t_{re} = T_e \cdot ln(9). \tag{3.14}$$

The system bandwidth α_c can thus be expressed as

$$\alpha_c = \frac{ln(9)}{t_{re}}. \tag{3.15}$$

The output current i of the closed loop system can be expressed as

$$i = F_c(s)G_e(s)(i_{ref} - i), \tag{3.16}$$

and the transfer function of the closed loop system G_{cl} can be expressed as

$$G_{cl} = \frac{i}{i_{ref}} = \frac{F_c(s)G_e(s)}{1 + F_c(s)G_e(s)} = \frac{\alpha_c}{\alpha_c + s} = \frac{\frac{\alpha_c}{s}}{\frac{\alpha_c}{s} + 1}. \tag{3.17}$$

where the transfer function of the electrical dynamics $G_e(s)$ of the RL-circuit depicted in Fig. 2.3 is

$$G_e(s) = \frac{1}{sL + R}. \tag{3.18}$$

Using the numerators of the equality in Equation (3.17) we have that

$$F_c(s)G_e(s) = \frac{\alpha_c}{s}. \tag{3.19}$$

Combining Equation (3.18) and (3.19) the controller $F_c(s)$ is

$$F_c(s) = \frac{\alpha_c}{s}G_e^{-1}(s) = \frac{\alpha_c}{s}(sL + R) = \alpha_c L + \frac{\alpha_c R}{s} \tag{3.20}$$

where the PI-controller parameters can be identified as

$$K_p = \alpha_c L, \quad K_i = \alpha_c R. \tag{3.21}$$

The electrical dynamics of the system is decided by the filtering inductance. The filtering inductance is 5.2 mH per phase and its inherent resistance is 173 mΩ. The rise time t_{re} is chosen to be 1 ms. From these parameters, the regulator parameter values is calculated to be $K_p = 380.1199$ and $K_i = 11.4256$.

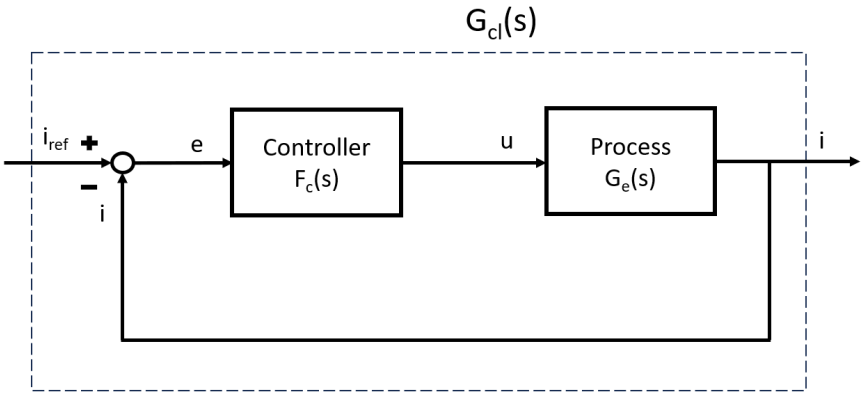

Figure 3.5: Block scheme representation of a general ideal closed loop system.

3.1.4 PWM Generation

The controller output signal is scaled down by half the dc voltage supplying the inverter bridge which results in the control signal $V_{control}$. The control signal $V_{control}$ is compared with a triangular waveform $V_{triangle}$ with peak-to-peak value of 2. It is the triangular

waveform that establishes the inverter's switching frequency. The switches on the positive side T_{A+} and the negative side T_{A-} of the bridge open and close according to the comparison of the wave signals.

$$\begin{aligned} V_{\text{control}} > V_{\text{triangle}}, \quad & T_{A+} \text{ is on} \\ V_{\text{control}} < V_{\text{triangle}}, \quad & T_{A-} \text{ is on} \end{aligned}$$

The output of the inverter is square waves of varying width that need to be filtered into sinusoidal AC waveforms.

3.2 Filter Design

Filters are required to obtain sinusoidal AC voltage and current output. This section describes the design and evaluation of different filters suitable for the application.

3.2.1 Filter Options for Voltage Based Inverter

The output signals of the three phase PWM inverter exhibits characteristics of pulsed waveform, owing to the 10kHz switching frequency seen in Fig. 3.7b. The switching introduce frequency components beyond the desired 50Hz fundamental frequency, hinted in Fig. 3.7a. These additional frequencies are deemed undesirable. To mitigate their influence and isolate the fundamental sinusoidal frequency, a filtering process is imperative. To exclusively extract the fundamental frequency, a low-pass filter is employed.

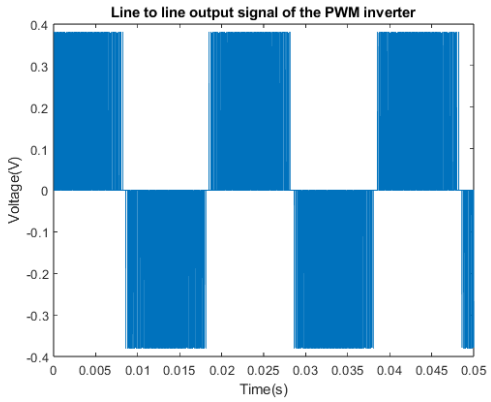

(a) Output of PWM-inverters.

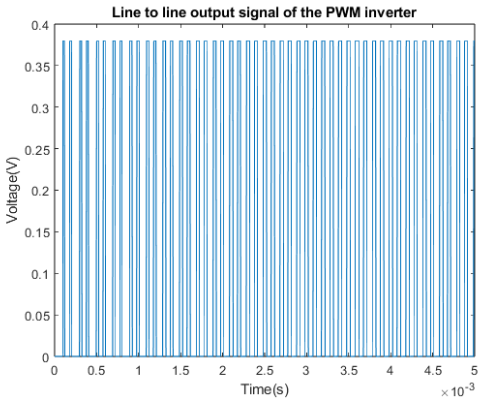

(b) Zoomed in output of PWM-inverters.

Figure 3.6: Output phase-to-phase signal from PWM-inverters in different with different zooms.

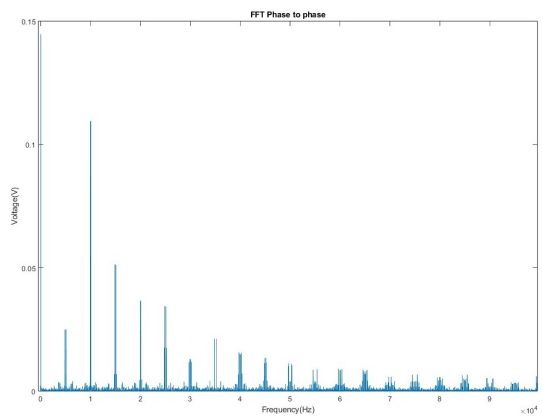

(a) FFT of phase to phase

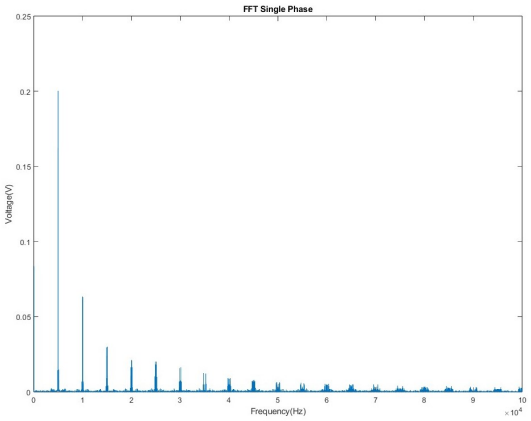

(b) FFT of phase to ground

Figure 3.7: FFT of the output voltage with no filtering

From the FFT plots it can be seen that there is a considerable amount of harmonics from the switching frequency. The phase-to-phase plots shows better results as the third harmonic is of the same frequency and amplitude but not the same phase and that means the third harmonic from two phases will take each-other out.

3.2.2 LCL-Filter

Initially, a proposed LCL filter configuration, comprising two inductors in series with a capacitor connected in parallel between them (see Fig. 3.8a), was examined to determine its effectiveness in filtering the output voltage.

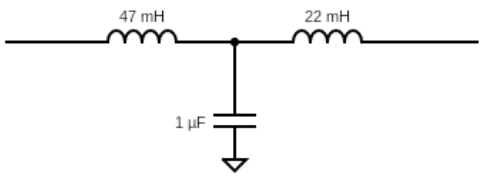

(a) Circuit of the proposed LCL filter.

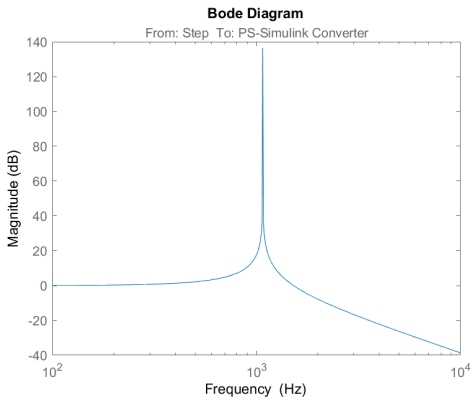

(b) Bode plot of the LCL filter.

Figure 3.8: The LCL filter design and bode plot.

From the results, one can observe that the LCL filter will attenuate the higher order components such as the 10kHz switching frequency of the inverter, see Fig. 3.8b. The filter will also greatly enhance signals at around the cutoff frequency as it is the resonance frequency of the circuit which will lead to a near zero-ohm resistance. To mitigate the risk of ending up in the frequency range where the signal is greatly enhanced as the signal frequencies might fluctuate during tests, other filter approach is to be examined.

3.2.3 Damped Filter

For the voltage-based inverter, a sinusoidal signal is needed to replicate the grid voltage characteristics. A damped filter is implemented to filter out the high frequency disturbances. The filter consists of a series inductance with two capacitor in parallel and a resistance and inductance in series with one of these capacitances, see Fig. 3.9. The LC circuit on the left-hand side of Fig. 3.9 is used as a low pass filter to filter out higher order unwanted frequencies, similar to the LCL-filter in section 3.2.2. In turn, the RLC circuit on the right-hand side of Fig. 3.9 is in place to dampen the resonance caused by the LC circuit. The damped filter was simulated in Matlab using the transfer function and creating the bode plot to visualize the cutoff frequency of the filter, see Fig. 3.10 [8].

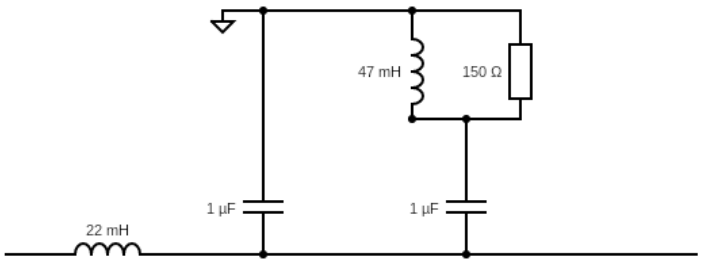

Figure 3.9: Circuit diagram of the damped filter. Shows filter applied per phase

Component values was approximated first using simulations first then changed so that harder to get components would be prioritized and then rest of the components chosen so that the model would fit. The data was then exported to Matlab where a FFT could be performed to see how much of magnitude of the switching frequency was left after filtering.
To find a capacitor which could perform AC filtering for higher voltages while also the impedance being able to remain relatively unchanged during higher frequency, a safety capacitor was deemed that it was usable because of their filtering and safety properties which makes them good for this projects as they meet the demands for the project. A safety capacitor is a type of capacitor which if it were to fail it would create an interruption in the circuit causing the flow of current to be ceased, this is the reason safety capacitors are often used in industrial settings as they can meet the safety regulations. The safety capacitor is split up to different classes determining the use and voltage range of the input into the capacitor. The types X and Y denotes how it is configured between the phases where X is used so it is put in between the phases whilst Y is from phase to ground. Type Y was then deemed more appropriate to use in this project because the filter would be installed to each phase and not interconnected between the phases. The number rating goes from 1-4 and determines the magnitude of voltage the capacitor have to handle. As the number ratings of these capacitors go quite high a lower number would be sufficient for the project to use. As safety capacitors are less used than the common electrolytic capacitors that means that the supply is less and there would be less options on these on the market. One of the big hurdles would also be the ratings of the magnitude

in the capacitors as the safety capacitors only have a relative low rating then the rest of the circuit would need to compensate so that the cutoff frequency off the transfer function would be at a desirable spot. The highest value for a Y-type safety capacitors available on the market were 1μF and had a Y2 rating. The rest of the components were chosen so that the values would match with the transfer functions bode plot and that the components would remain constant even at higher frequencies. [9]

For the rest of the components there was a greater supply of different components which could be used. The criteria for the rest of the components were the same as before that they would need to have a voltage safety threshold a bit higher than the rated voltage and that the values would remain constant for frequencies in the kHz range. Two different types of radial inductors for the series and parallel filtering for each phase of the filter as well as a film resistor were deemed suitable for this application. The values of the components are summarized in Table 3.1.

Components	**Value**	**Amount**
Capacitor	1 µF	6
Inductance series	22 mH	3
Inductance parallel	47 mH	3
Resistance	150 Ω	3

Table 3.1: Components for filtering

The following circuit could be converted to a transfer function. By utilizing Matlab Simulink, the transfer function could be calculated to the following:

$$G(s) = \frac{0.001045 \cdot s^3 + 4.545e7 \cdot s^2 + 3.03e11 \cdot s + 9.671e14}{s^4 + 1.333e4 \cdot s^3 + 8.801e7 \cdot s^2 + 3.03e11 \cdot s + 9.67e14} \tag{3.22}$$

With the transfer function at hand the circuit could be presented by a bode figure to find out how the circuit will act under different frequencies.

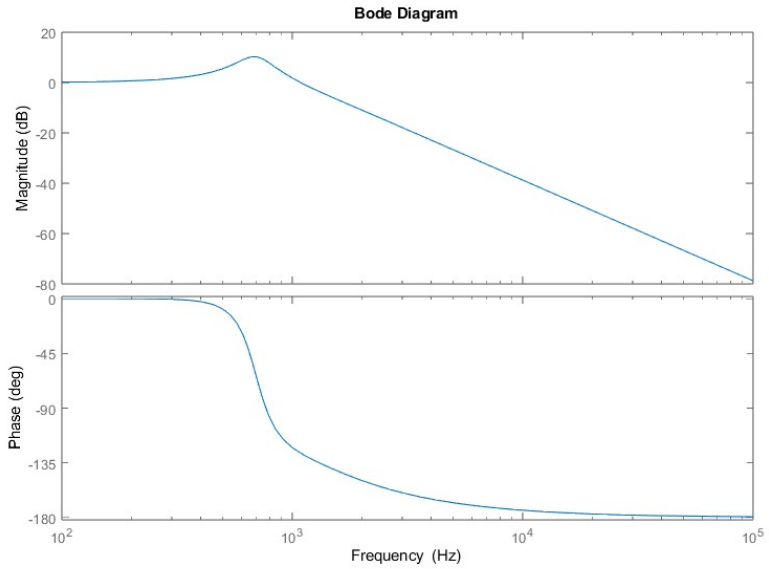

Figure 3.10: Bode plot of the transfer function from the damped filter

By analyzing the bode plot from the transfer function a couple of results could be observed. The frequencies below around 800Hz remains relatively unaffected by the filter meaning our fundamental frequency of 50Hz would be able to pass through unaffected. The cutoff frequency is at around 1kHz which will mean that higher frequency components than 1kHz will be damped to some degree. Here we can also see the effect of the damping circuit as the resonance frequency is not quite as big as for the LCL case. The 10kHz switching frequency of the inverter will be damped by -38.9 dB.

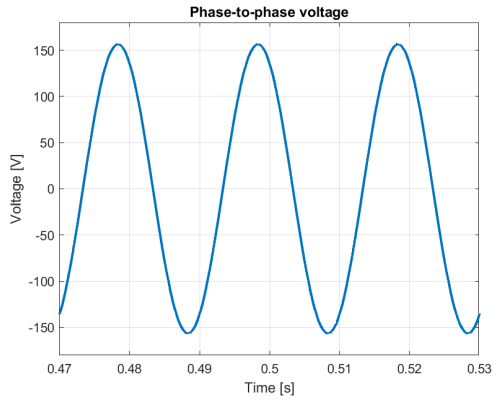

(a) Phase to phase voltage of the output of the filter.

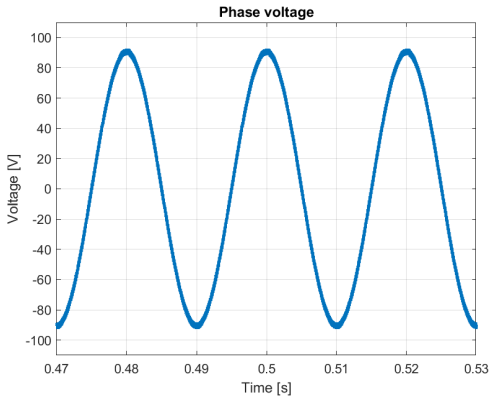

(b) Single Phase output of the output filter.

Figure 3.11: Phase-to-phase voltages and phase voltages after filtering.

By looking at the different voltages the phase-to-phase voltages experience a lot less ripple caused by the switching of the PWM-inverters. This could be because the ripple is caused by a 0-sequence harmonic component. The 0-sequence has the property that it has

the same amplitude and direction in each of the phase. This means that the 0-sequence component will extinguish each self when checking the phase-to-phase voltage.

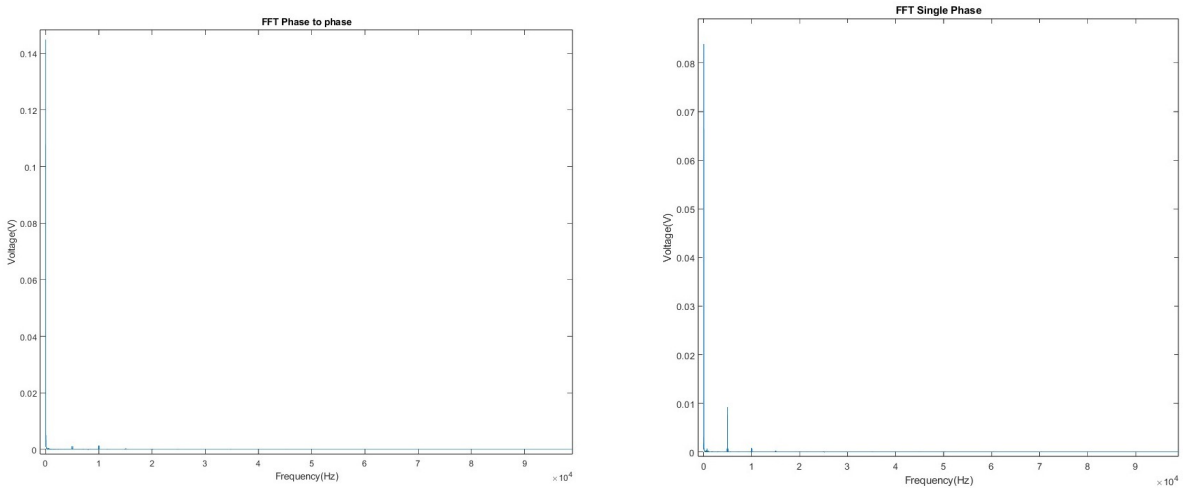

(a) FFT phase to phase after filtering **(b)** FFT phase to ground after filtering

Figure 3.12: FFT plots of output voltage after filtering

This can also be observed in the FFT plots in Fig. 3.12. For the phase to ground a bigger harmonic component can be observed at 5kHz while at the phase to phase the harmonic content is mostly eliminated because of the it is a third harmonic component leaving only a pure sinusoidal signal at 50Hz.
Filter tests were done by utilizing one of the converter bridges at low voltage to analyze the form and amplitude of the voltage after the damped filter. .
To finalize the filter and make it easier and safer to use, a CAD schematic was created for the filter. The filter was modeled in KiCad, an online tool for creating circuit boards and was implemented and fitted using the dimensions of the components for the filter.

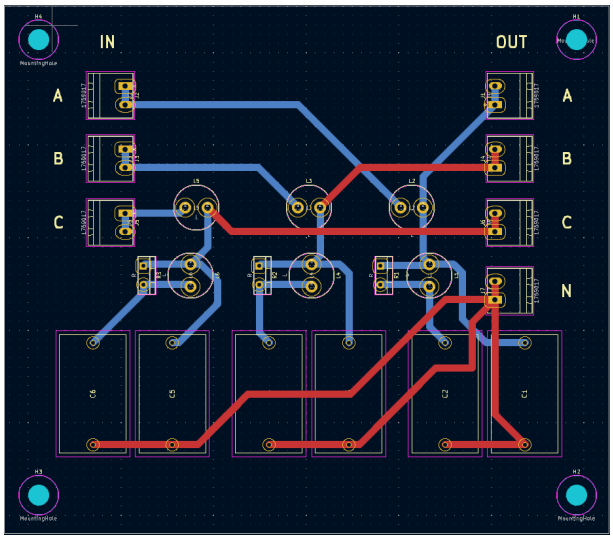

Figure 3.13: Footprint and routing of the filter.

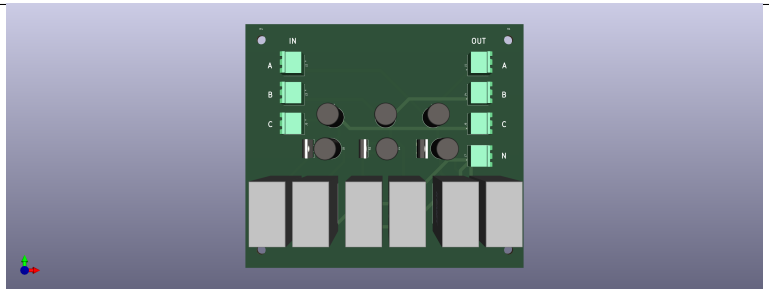

Figure 3.14: 3D model of the CAD layout.

To check the voltage drop over the filter the simplest way to do so is just to measure the voltage when the converter had a set value and see what the voltage difference is between the set value and the actual value. Using an oscilloscope, when the voltage reference value was set to $110V_{rms}$ the output of the filter showed a magnitude of approximately $109.3V_{rms}$ meaning a $0.7V$ voltage drop from the filter. Even when used on lower voltages for example $24V_{rms}$, then the filter voltage dropped was showed to be consistently even during these tests as well meaning that it could be compensated easily in the code by adding $0.7V$ to the reference voltage value.

3.2.4 Filtering of Current Based Inverter

For the current based inverter, it does not need to have as clean sinusoidal output voltage as the voltage-based converter because we only want a good sinusoidal current and can therefore utilize a simpler filter with less components. The current based inverter has to have a good output current and a single indicator per phase is sufficient enough to filter out the higher frequency components. After filtering a signal which mostly consist of a sinusoidal fundamental frequency is in place but with further probing the signal has quite a ripple on it. To minimize the ripple of the output, current a further investigation of the output inductance takes place. Another limiting factor choosing a components for filter were the current ratings. A maximum of 5A output from the inverter which is quite high for many of the inductors on the market. A 3-phase inductor where each phase is connected to a single component was chosen as it had a high current rating of 10A as well as a constant inductance at the frequencies the switches operate at.

3.3 Working Connections for the Voltage Regulating Inverter

Two different setups of the voltage regulating inverter was built to consider the best solution to supply stable 110 V_{rms} at desired frequency. The first solution utilized 380 V bridge output that is filtered into the desired 110 V_{rms} AC signal. The second solution utilized a low voltage bridge output that was filtered and then the voltage were transformed up with the help of a transformer with a 1:40 ratio into the desired 110 V_{rms} AC signal.

The open loop voltage inverter block diagram for the setup without transformers can

be seen in Fig. 3.15. The rectifier is supplied by a 230 $V_{phase,rms}$ source, which in turn supplies the half-bridge. The half-bridge creates square waves that is filtered into the desired 110 $V_{ph-ph,rms}$ signal. Fig. 3.17 depicts the block diagram of the setup utilizing transformers to step up the voltage to the desired magnitude. The laboratory connections for both setups can be seen in Fig. 3.16 and 3.18.

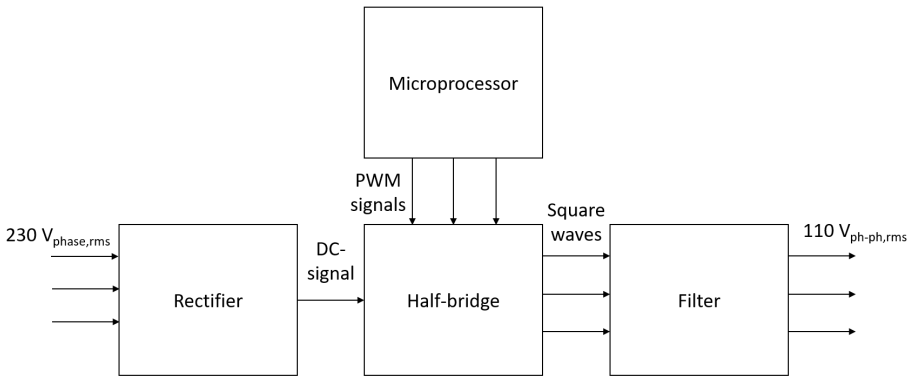

Figure 3.15: Block diagram of the voltage inverter scheme without transformers, "high voltage bridge solution".

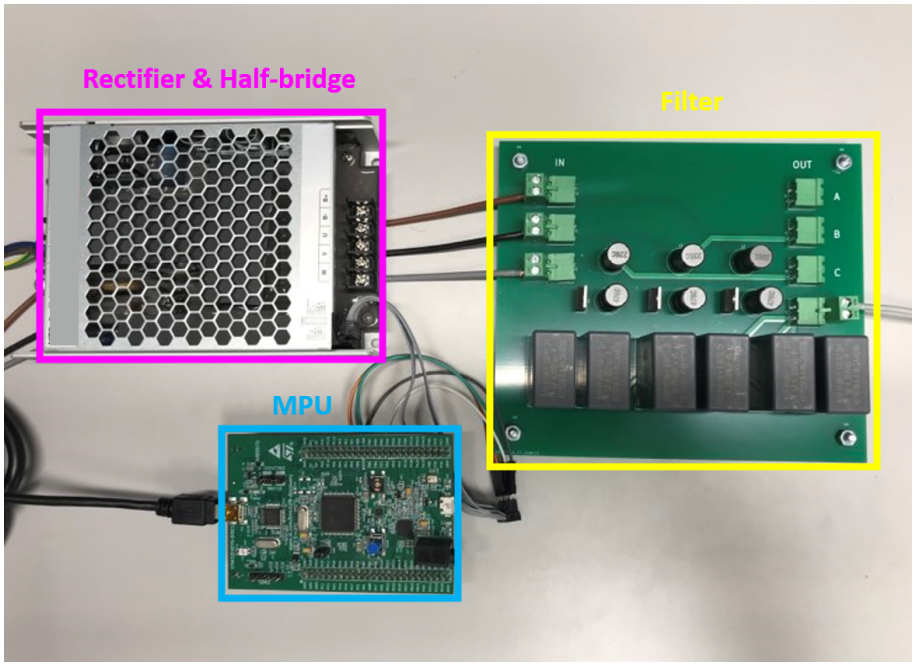

Figure 3.16: The laboratory circuit of the voltage regulating inverter without transformers.

For the use of transformers, a circuit was created which would test how they would perform to the higher voltage converter to see if the performance of this setup would be of equal if not more beneficial than just using a higher voltage converter. One advantage of utilizing transformers is the possibility to use the smaller DC supplied half bridge, taking

less space in a final product. The main advantage however, is that the transformer solution enables the usage of batteries supplying the half bridge as contrast of the bigger half bridge solution requiring wall socket supply. HzOn (the testing equipment) is already equipped and supplied by a battery, therefore the transformer solution would not require a lot of extra components. During tests using the product, the batteries eliminate the risk that unstable voltage supply would compromise the test results.

However, the high voltage bridge solution is still relatively compact, and the advantage is that there is less components while having good performance in terms of creating stable and balanced output signals at different frequencies. Including transformers could cause additional complications if not handled correctly. First and foremost is to find and use adequate transformers which would be able to clear the maximum desired voltage and additionally be rated a bit higher than that to get a safety margin. The transformer should also not be saturated and preferably not close at all to saturation when the circuit runs at maximum voltage because at saturation then the transformers will not increase the voltage linearly anymore and will subsequently show values which differ from the theoretical circuit by quite a margin.

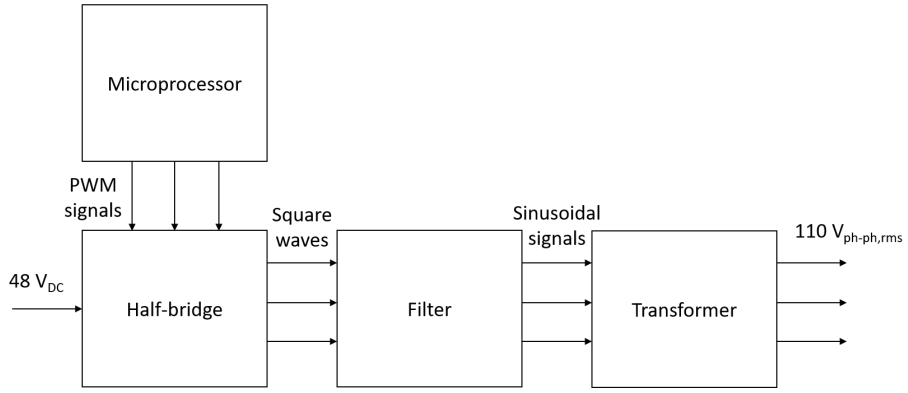

Figure 3.17: Block diagram of the voltage inverter scheme including transformers, called the "transformer solution".

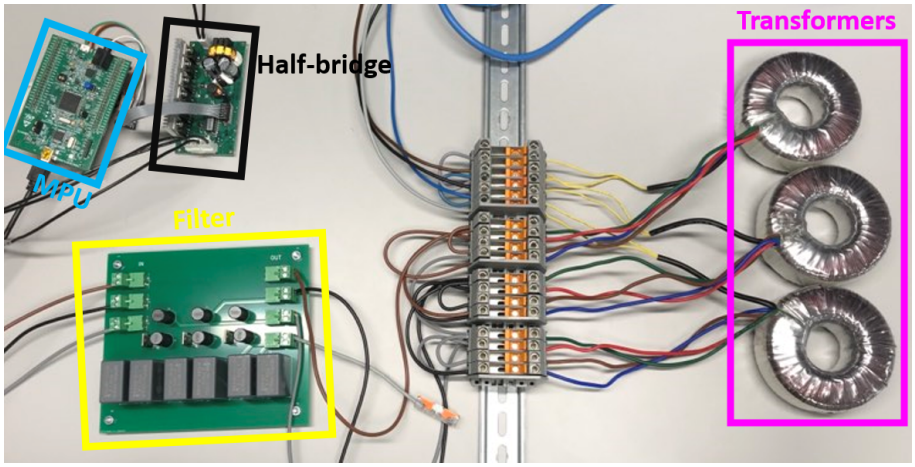

Figure 3.18: The laboratory circuit of the voltage regulating inverter with transformers.

The transformer solution utilized the same filter as the high voltage half bridge solution utilize to obtain the fundamental sinusoidal AC signals. Tolerances in the components of the filter may cause imbalance in the phases resulting in different voltage magnitude or phase shift. In the transformer solution, the imbalance may be relatively big compared to the high voltage bridge solution. The voltage drop over the filter is the same for the two solutions in absolute terms. If the voltage drop differ between phases due to the tolerance of the components, and then the voltage being transformed, then the amplitude error will also amplify. Besides, disturbances on the low voltage side of the transformers due to DC-supply or interference may also be amplified causing trouble. Further work should be performed to design suitable filters for respective half bridge solution.

3.4 Working Connections for the Current Regulating Inverter

The current regulating inverter is coupled as depicted in Fig. 3.19. The half bridge is supplied by a DC voltage and the output is square waves that is filtered into sinusoidal current wave forms. The AC current is measured and fed back to the microprocessor that calculates the PWM signals to obtain the desired AC current. The laboratory circuit can be seen in Fig. 3.20.

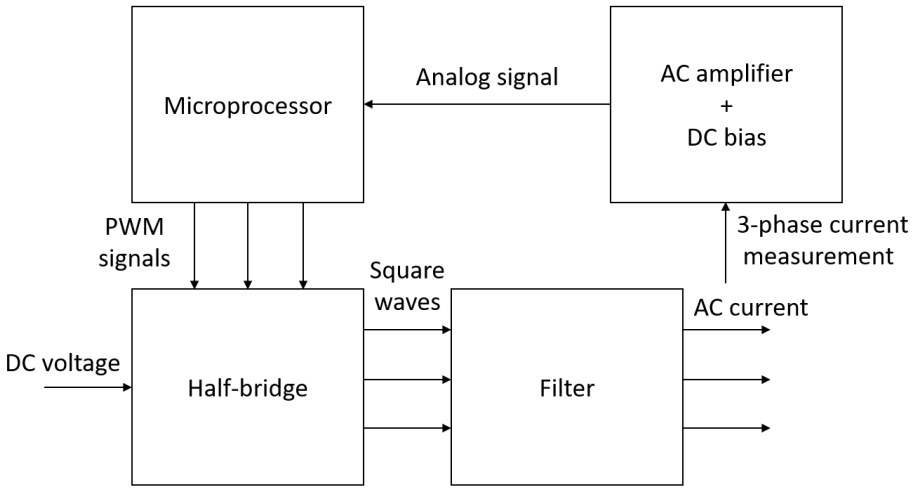

Figure 3.19: Block diagram of the current inverter scheme.

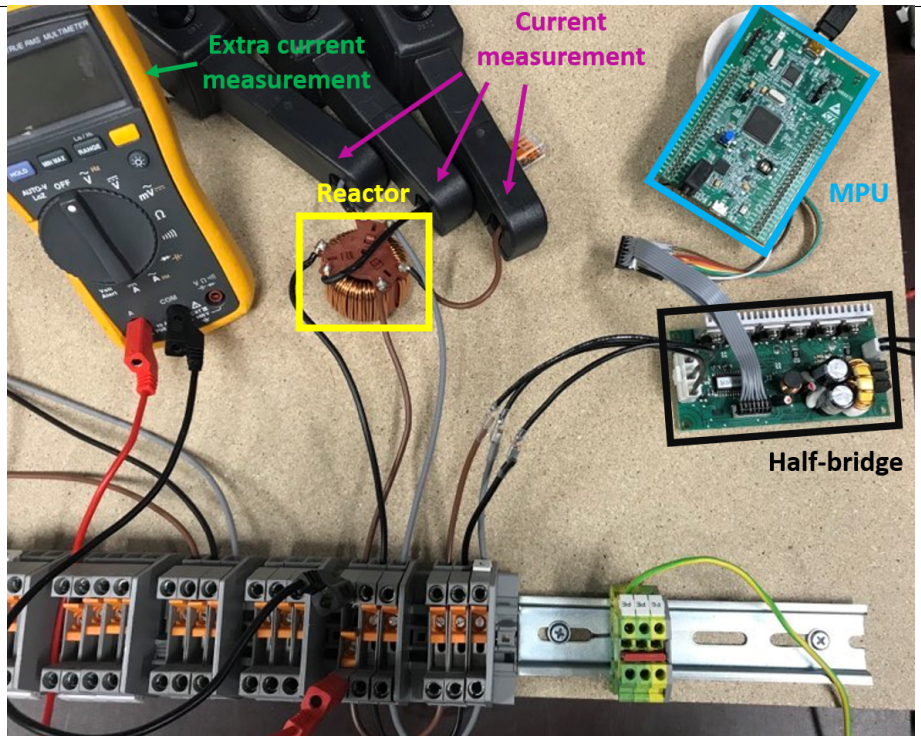

Figure 3.20: The laboratory connections of the current regulating inverter.

The current probes measure the current of each phase. The analog input port of the MPU accommodates voltages ranging from 0 V to 3.3 V, corresponding to 4095 bits in the analog to digital converter (ADC) of the MPU. Each current probe provides a sensitivity of 1 mA/ 1A. These probes are connected to a 10 Ω resistance, allowing for a measuring range of 50 mA to 90 A in this configuration. The voltage across the resistance, representing the current in the circuit, is connected to the analog input port of the MPU. The voltage signal representing the current is one hundredth of the current amplitude due to the sensitivity of the current probe and the 10 Ω resistance according to ohm's law. The current in the converter will range between 0 A and 5 A RMS, meaning the maximum current peak value will be represented by 70 mV on the ADC ports. The resolution of the ADC is,

$$\text{Resolution} = \frac{\text{Voltage range}}{\text{Number of discrete values}} = \frac{3.3\text{ V}}{4095\text{ bits}} \tag{3.23}$$

, resulting in approximately 0.8 mV/bit.

Problem occurs when the current measured is AC which means half the period is negative. The microprocessor is only able to measure positive voltages which means AC will only register half the period and the negative part of the period will result in a 0 V measurement which is simplified and illustrated in Fig. 3.21. To bypass this problem a DC offset voltage is applied to the AC signal. The DC offset should bias the signal to the middle of the MPU's analog input port voltage range, allowing the AC signal to be as large as possible.

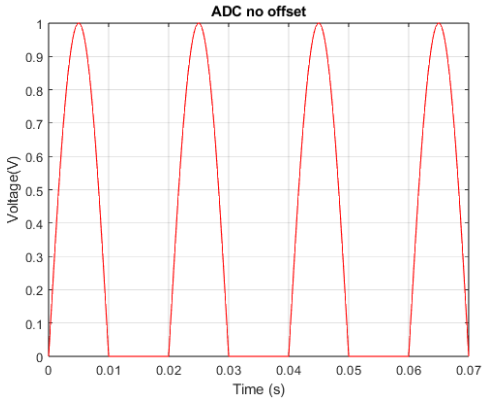

(a) ADC input signal without using any offset

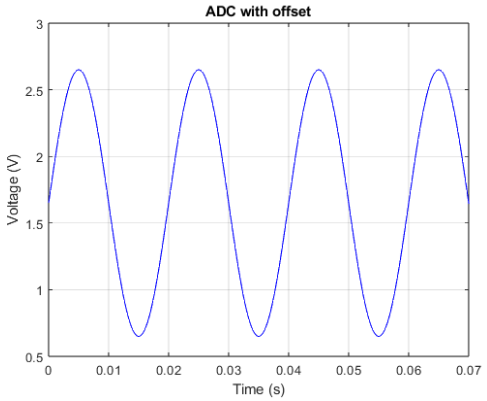

(b) ADC input signal with an offset

Figure 3.21: Difference of ADC signal with or without using an offset

Adding an offset of 1.65 V will allow the AC signal amplitude to be 1.65 V_{peak}. If the AC signal is not amplified, maximum 4 % of the voltage range will be used, resulting in bad resolution. To amplify and DC offset the AC signal, an operational amplifier was used according to Fig. 3.22. The voltage divider in the op-amp circuit, consisting of resistors R3 and R4, provides a 1.65 V offset when the two resistors have equal values. The gain of the op-amp circuit is determined by

$$\text{Gain} = -\frac{R2}{R1} \tag{3.24}$$

. This circuit enables full range AC signals and improved measurement resolution.

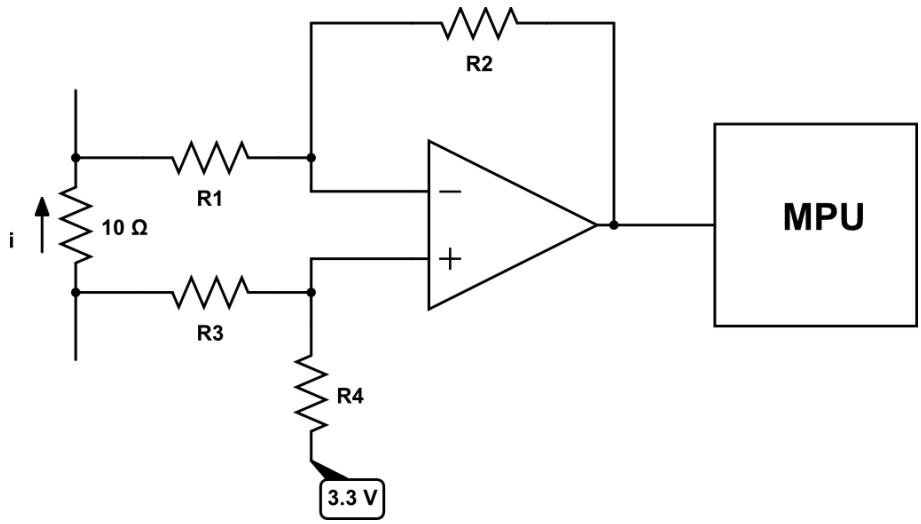

Figure 3.22: Operational amplifier-circuit to amplify and DC offset the AC signal.

4

Transducer Impact on Testing

To be able to test the power generating facilities that they function as they should then the transducers there are requirements on the transducers. The requirements can be summed up to that the signal inserted into the transducer needs to convert to the system as fast as possible. For testing purposes, the signal mostly consists of frequency, current and power which are first given as digital signals were the transducer then converts them into analog signals to the system.

The focus on this study is to check the importance of the transducer during testing of generators by modeling and changing different parameters to simulate different types of transducer models.

The study included checking two different systems, one hydro station to simulate slower systems and one battery storage system to simulate faster systems and to see if it had any impact based on the system speed.

4.1 Transducer Impact on a Hydro-Power Station

In the power station modelling the frequency is fed back to the reference signal to compare the difference between the reference and after the hydro power station. To test the transducer the feedback loop is broken up whereas a substitute signal is put into the comparison which is controllable and can be altered during the test instead of the feedback signal. Then different signals can be inserted to see the response of the power station during different conditions. A hydro model is then used to see if there is any greater impact utilizing different transducers. The hydro model stations are a simplified version of a real hydro station consisting of a servo, penstock, turbine, a PI controller and feedback for the active power which is dependent on the difference in frequency between the reference 50Hz and the grid frequency which is the substitute frequency. There is also a droop to give the frequency some margin. The model also implemented dependence on the RPM of the turbine with the constant D_t but this was not used in this model and was put to a value of 0 to make the system undependable on it. To check that it complies with the requirements for FCR the results are compared to the criteria for FCR delivery on which Svenska Kraftnät has brought forward.

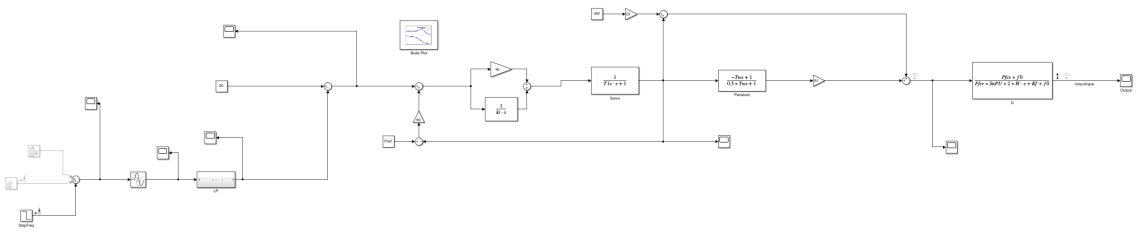

Figure 4.1: Simulink hydro power plant model for transducer testing

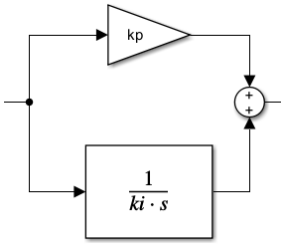

(a) PI controller block

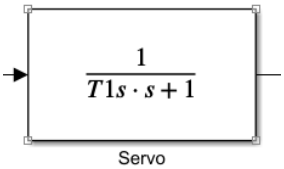

(b) Servo block

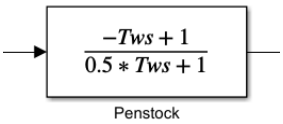

(c) penstock block

Figure 4.2: Different blocks used to represent the a hydro power plant in Simulink

By utilizing this model of a hydro power station one can implement a model of the transducer in Matlab Simulink to test these abilities and see how they can affect the machine during testing. To model the transducer there are different ways to model it with how it will act which is also dependent on the model of the transducer. The transducer can be modeled with a low pass filter to replicate the step-up time, with a delay to replicate the time it takes to react or with both.

Figure 4.3: Model representation of a transducer in Simulink

For modelling the transducer in Simulink then it was modelled of blocks consisting of a delay and low pass filter. The input signal is given as a step-in frequency with 1Hz deviation from the 50Hz standard. For the delay it can be modelled according to the following equation:

$$Y(s) = e^{-st} \tag{4.1}$$

, where t is the delay time. The ramp up time modelled as a low-pass filter can be defined

as:

$$G(s) = \frac{1}{sT + 1} \tag{4.2}$$

where T is the time constant of the lowpass-filter. Combining the two would result in the following equation:

$$H(s) = G(s) \cdot Y(s) = \frac{e^{-st}}{sT + 1} \tag{4.3}$$

4.1.1 Testing of Different Transducer time constants

To see if a slower transducer would affect this slower type of power system, then a transducer was implemented with varying degree of speed to see the effect on the system during testing. Utilizing Matlab and Simulink on a hydro-power plant model different conditions were implemented to simulate the effect different transducers had during testing. The test consisted of modelling the transducer as a lowpass-filter, delay and the combination of the two and when evaluate the response. The result was evaluated using a bode diagram from the system and see the response. Changing the integrator time constant T in the lowpass-filter to model the speed of the transducer and see how different transducers can affect the speed of the generator output. The tests on the transducer were based on the official requirements for testing of FCR-N on generators by Svenska Kraftnät [10]. Utilizing first a frequency step response by a step from 50Hz to 49Hz and changing the value of parameter T in the low pass filter and see how it affects the speed of the generator output. As it only affects the ramp up the picture is zoomed in, and the power saturation is cut out.

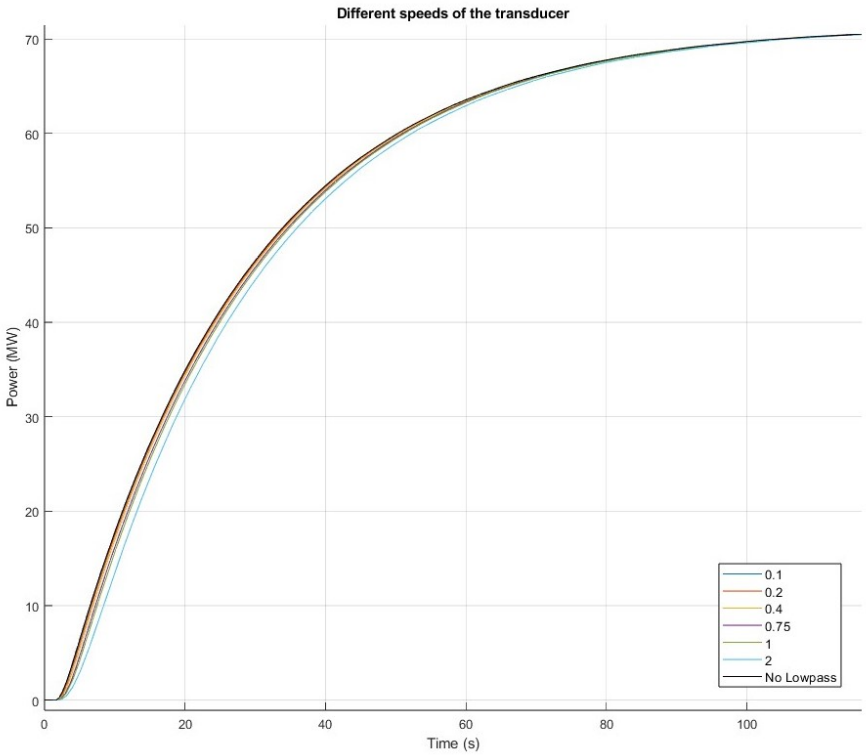

Figure 4.4: Different speeds of transducers for the hydro model.

A bode plot tells more information. The bode plot shows that for higher speeds then there would a bit of filtering effect of signals of frequency higher than 10^{-3}Hz. As for the delay it only affects signals under 10^{1}Hz and because the system works mostly on the fundamental 50Hz that remains unaffected.

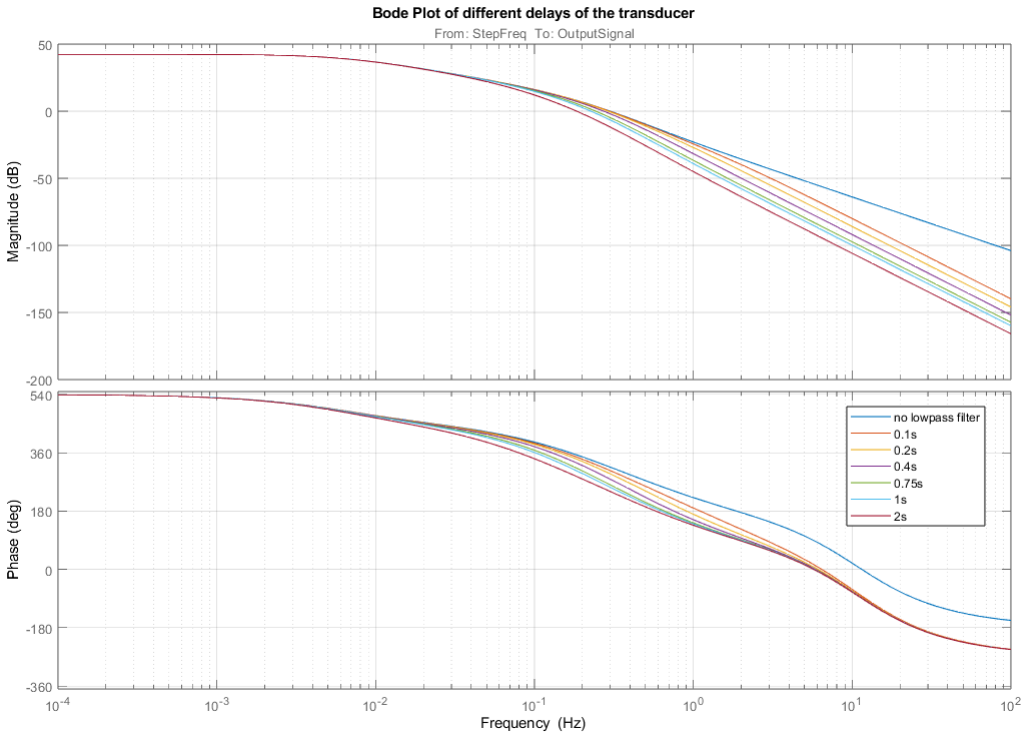

Figure 4.5: Bode plot of different transducer speeds.

The range of values for the speed of the transducers were of typical values where higher values would represent older and slower transducers and lower value model the newer and faster transducers, the biggest value of 2s were of a more extremer case to showcase which values of T would cause a greater deviation from the no lowpass-filter case. From the results it could be observed that the impact of fast and slow transducers was not of high degree, which means that during testing of generators it would not matter greatly what type of transducer is installed in these facilities of we only regard the speed of the signal transformation.

4.1.2 Transducer Delay

For the delay then different values were tested for the transducer to see if it had any effect on the system. While transducer delay can very, they all are typically fast with a delay under 1s at least. The tested values were 20ms, 50ms 100ms and 1000ms where the last value is a bit of an outlying value to check if there were any noticeable difference at a much higher delay. As for the system in Simulink can not linearize the e^{-st} as the transfer function is that it is not a rational function which Matlab requires to be able to linearize the model, then it needs to be approximated. Within Simulink the delay can be approximated instead utilizing Padé approximation of different orders, the

higher the order the more complex but more terms are added to represent the function. The delay was modeled using the transport block in Simulink with a second order Padé approximation of the delay so the model could be linearized for the bode plots. Mostly lower order is used that's why an second order approximation was deemed sufficient to represent the delay in the model with high enough accuracy. From the bode plots it could be observed that there is some phase shift happening in the span of around 10^{-1} —10^{2}Hz while it remains constant for ranges outside it but in this range is where the fundamental 50Hz frequency exists meaning there will be a phase shift depending on the size of the delay from the transducer.

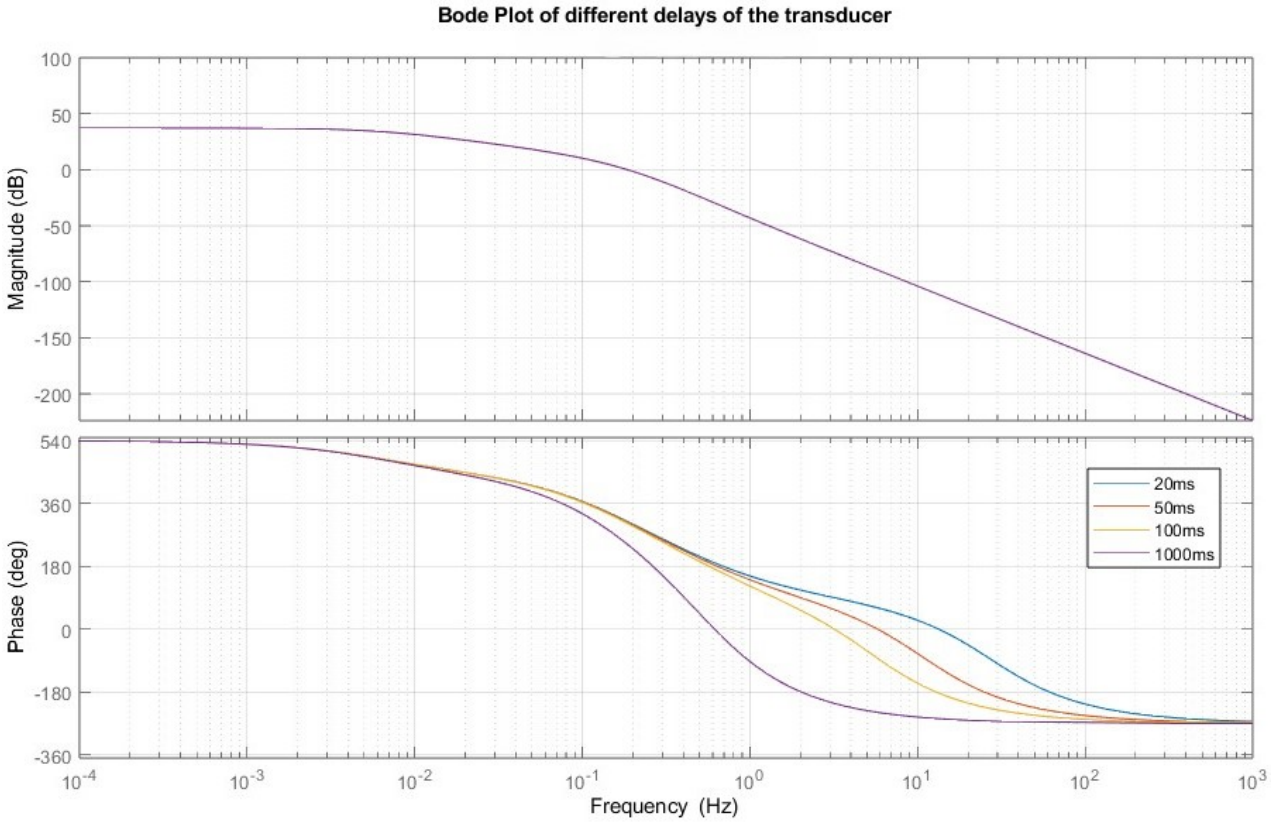

Figure 4.6: Bode plot for different delays.

4.2 Transducer Impact on a Battery Storage System

The previous tests were conducted with a hydro power plant which is a very slow system with a lot of delays. If instead the transducer were implemented to a faster system, then a more significant could appear. A model of a battery storage unit with which is a lot simpler than hydro power station as it only contains one transfer function compared with the hydro-power stations two.
For the battery model it is a simplified version of the hydro model. The waterworks and turbine are removed and instead fitted with a single transfer function with the aim to

model FCR provided by the battery.

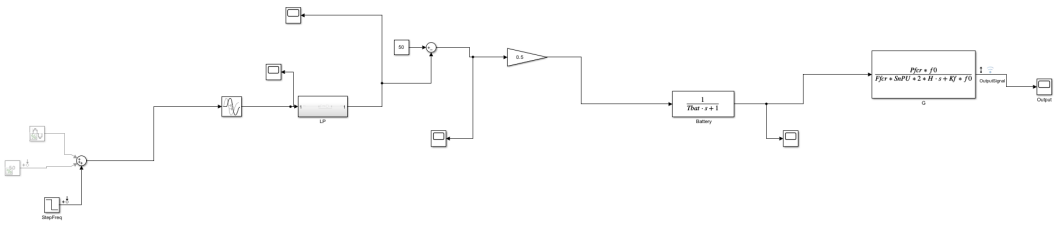

Figure 4.7: Simulink battery power plant model for transducer testing.

The biggest change is in the feedback and the PI regulator which are removed as it weren't needed in this case. Instead a block is added to get out the power variation from SVK's website [11]. The value of the block is taken from the calculation below:

$$|\Delta P| = 100 \cdot \frac{|\Delta f|}{50} \frac{P_{ref}}{s} \tag{4.4}$$

Where ΔP is the needed power to boost the frequency, Δf is the difference in frequency from 50Hz. The s is the droop of the system and is 4 % in this case. The P_{ref} is the reference power and the system is defined in per unit means the reference is just 1pu. The Δf comes from the incoming signal so only known values are left which gives a product of 0.5 and is modeled as a gain.

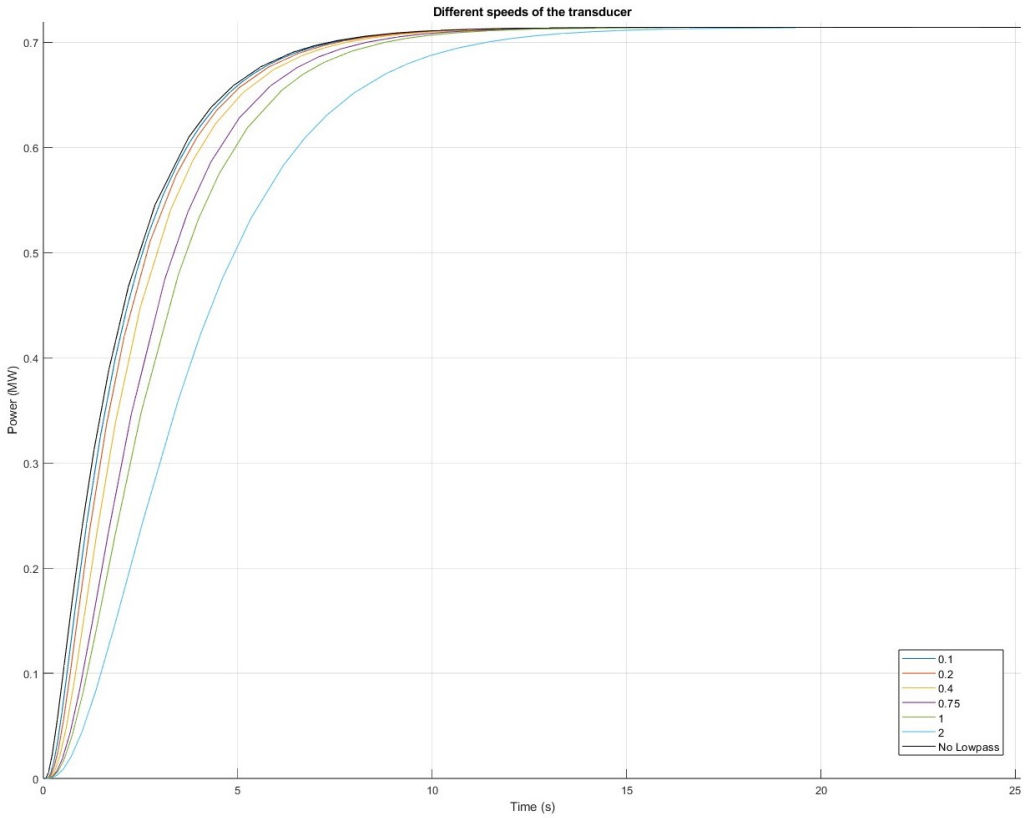

Figure 4.8: Speed of transducer in battery model.

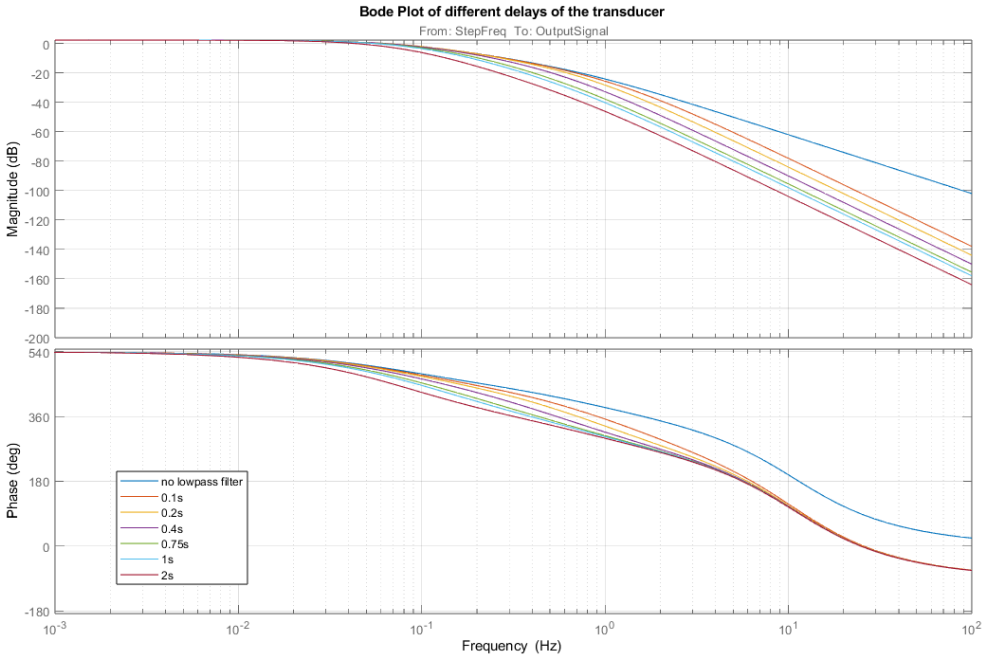

Figure 4.9: Bode plot of different transducer speeds using the battery model in Simulink.

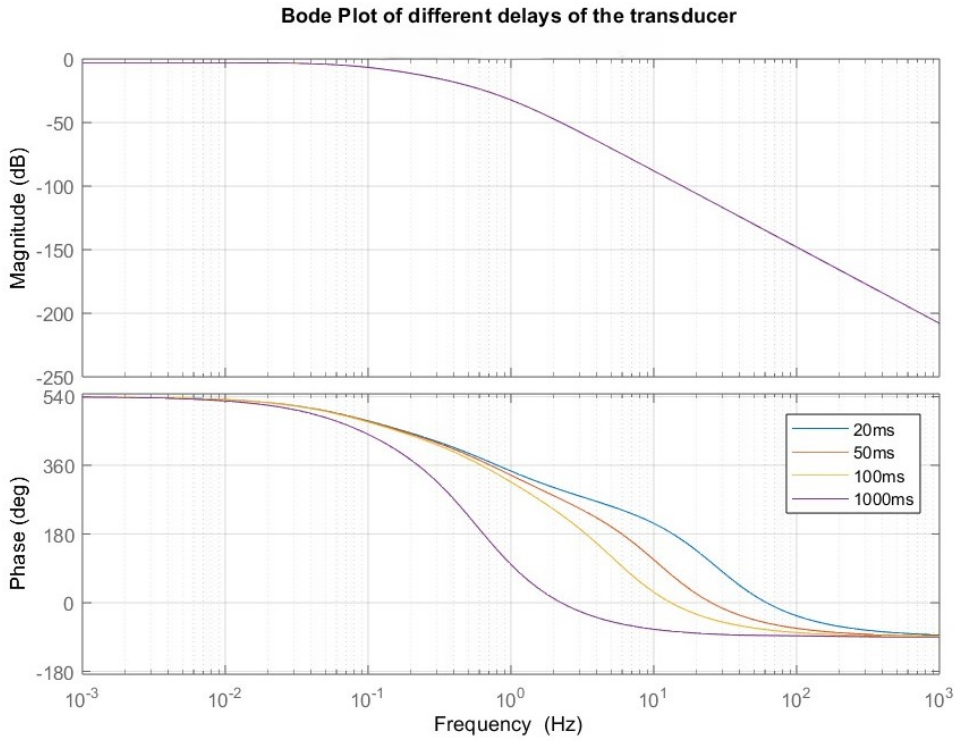

Figure 4.10: Bode plot of different delay using the battery model in Simulink.

To see if the transducer has any effect on systems with different response speed, then the test with transducer speed was rerun but with the battery model. The result from the test was quite similar that with relative low speed then the system. Compared with the speed of the transducer in the hydro model it could be observed that the transducer speed had a higher variation depending on the speed in comparison. This means that the transducer speed will have a higher impact on faster system, while for a slow system then the impact is quite small. Looking at transducers available then newer models have a response time of around 100ms. Some can even go a bit faster to less than 100ms and some are slower at around 200ms. Speculating the response time for older models then they usually have higher values but never exceeding 1000ms. This would mean that if the speed of the transducers is below that of 1000ms then there would be a minimal impact from the transducer on the tests. Looking at the bode graph then it shows quite the similar results compared to the hydro model which means it will affect the two models the same amount for phase and amplitude. Checking for different delays on the battery system it can be seen that it looked very close to the same for the hydro model and it shows that the delay does not differ with how fast the system is.

4.3 Conclusion of transducer impact

For the different types of transducers in various types of power stations it can be seen that the characteristic of the transducer has minimal impact on testing purposes. While the results for the transducer speed constant showed that slower transducers have a bigger impact on faster systems than slower it can also be seen that the impact came mostly

from outlying values and that for smaller values which were more realistically used in real applications then the real impact could be deemed small or maybe even negligible. The delay showed no difference between the systems of different speed and showed low impact on 50Hz frequencies.

5
Performance Testing

5.1 PSCAD Simulation

In this section, the results from the PSCAD simulations of the whole system of both inverters are presented. Most results are presented in DQ-coordinates and includes the voltages, currents, active- and reactive power. The frequency is analyzed in abc-coordinates. All data is measured at the filter output.

To analyze the system stability and response to changes, each graph in this section represents the sequence presented in Fig. 5.1.

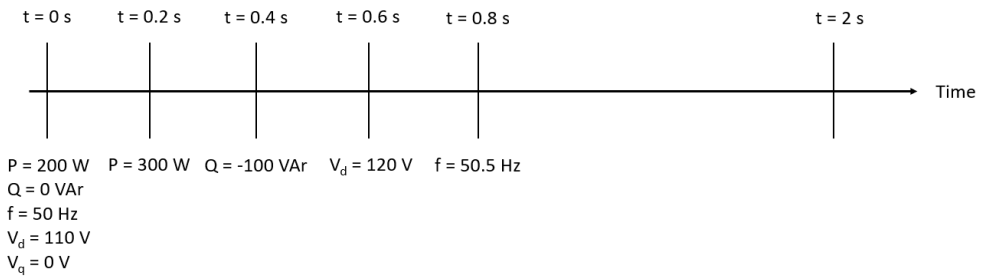

Figure 5.1: Variation of parameters along the simulation time. The initial values are set at t = 0 s. The parameters are not changed if not stated and hold the parameter value from its last change.

As can be seen in Fig. 5.2 the q-component of the voltage deviates from its reference value. Two different methods to get rid of the error was investigated. The first one called the Static Compensation compensates for the angle difference according to

$$\varphi = \arctan \frac{V_q}{V_d} \tag{5.1}$$

, where φ is the angle between the q-component of the voltage V_q and the d-component of the voltage V_d measured at 110 V_{rms}. The voltage is thus statically regulated to compensate for the angle φ.
The second method implies adding an integrating regulator (I-regulator) that reduces the error. For simplicity the bandwidth of the I-regulator is chosen such that $\alpha_{I-regulator} << \alpha_{filter}$ where α_{filter} is the cutoff frequency of the output filter of the voltage regulating inverter, so that the dynamics of the system can be assumed to be constant. The integral gain of the regulator K_i is thus the inverse of the time constant T. The integral gain K_i

is chosen to be 380 in the graphs below.

In summary, the different cases are defined as:

- **Base case** includes compensation for the ωL-term in dq-coordinates described in section 3.1.2 but still have some phase shift and thus introduce voltage in the q-coordinate.
- **Static compensation** includes compensation for the angle shift measured at 110 V_{rms}.
- **Active compensation** includes an I-integrator that reduces the voltage error.

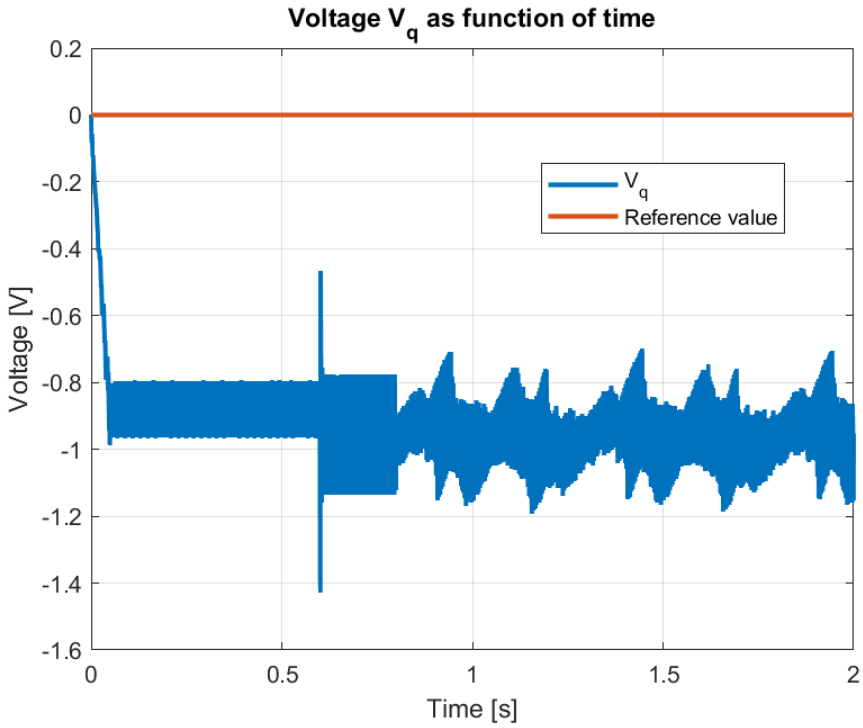

Figure 5.2: Q-component of the voltage deviates from the desired value of 0 V (reference value).

Fig. 5.3a depicts the result of the V_d static- and active compensation compared to the base case without any compensation. Fig. 5.3b depicts the voltage in q-coordinate for the three different cases. The oscillation of the voltage occurs after 0.8 s as the frequency is changed to 50.5 Hz, which is an uneven divider of the switching frequency of 10 kHz.

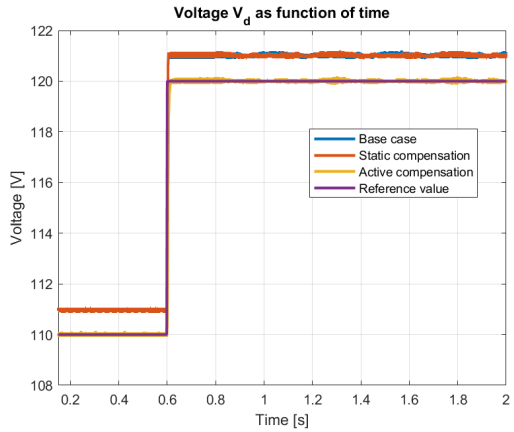

(a) Voltage V_d for the base case, static compensation, active compensation, and the reference value.

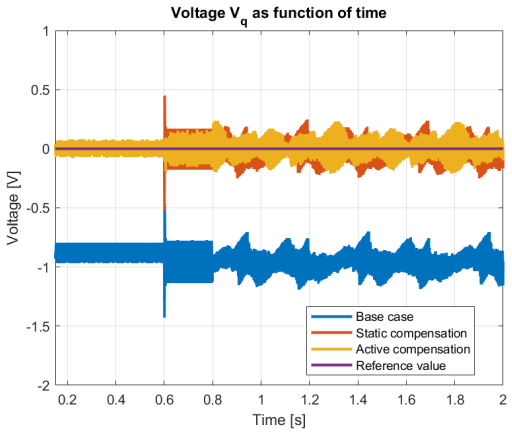

(b) Voltage V_q for the base case, static compensation, active compensation, and the reference value.

Figure 5.3: Comparison of V_d and V_q with their reference values.

Since the reference current is calculated from the desired power based on the assumption that $V_q = 0$ V and $V_d = 110$ V in Equation (3.1)-(3.2), it is important that the voltage components follow their respective reference value. Otherwise, the obtained power will differ from the desired value due to assumptions made in calculations that do not hold true. In the d- component of the voltage V_d, the active compensation case follow the reference value well, while the base case and the static compensation case deviates around 1 V from the reference value. The deviation can partly be explained by the filter having 0.0384 dB amplification at 50 Hz. In the q-component of the voltage V_q, the base case deviates from the reference value with around 0.9 V. The static and active compensation cases both follow the reference value in q-component voltage, implying the assumption made that $V_q = 0$ V is true while calculating the reference current.

Fig. 5.4 show how the d- and q-component of the current follow their respective reference value. The active and reactive power can be seen in Fig. 5.5. The active power consequently follows the reference value as a consequence of i_d and V_d does so. At 300 W active power reference value, the base case deviates 0.25 %, the static compensation case 0.5 % and the active compensation case 0.4 %, which means that the base case is the most accurate. The base case for the reactive power deviates from the reference value by around 3 % at -100 VAr reference. The deviation occurs probably due to the deviating q-component of the voltage V_q. The static and active compensation cases deviates 0.5 % each from the reference value of -100 VAr in reactive power. As a conclusion, the static and active compensation cases gives better reactive power accuracy than the base case. In active power, all three cases holds satisfactory accuracy. Therefore compensation, either static or active, is recommended. The disadvantage of active compensation is the necessity of measuring the voltage in a feedback loop, making the system more complex. The active compensation is however more accurate than the static compensation. No further accuracy optimization has been conducted except for the voltage compensation.

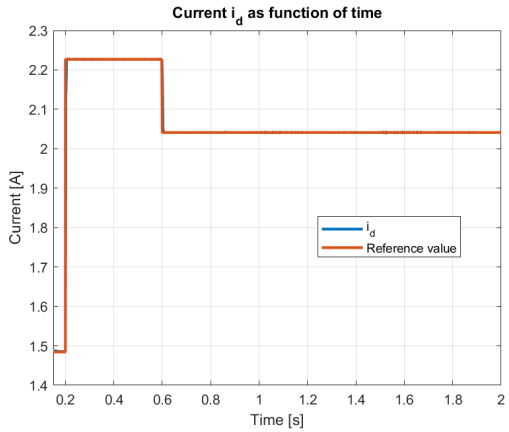

(a) Voltage i_d and the reference value.

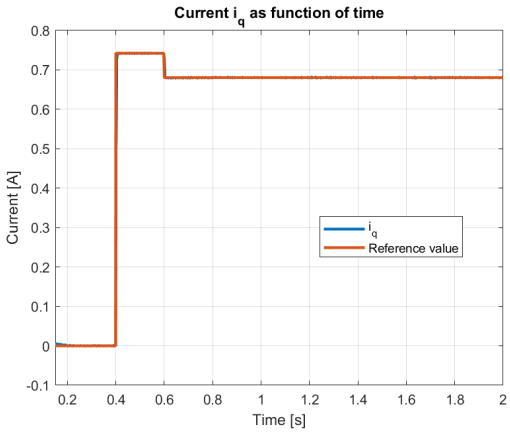

(b) Voltage i_q and the reference value.

Figure 5.4: Comparison of i_d and i_q with their reference values.

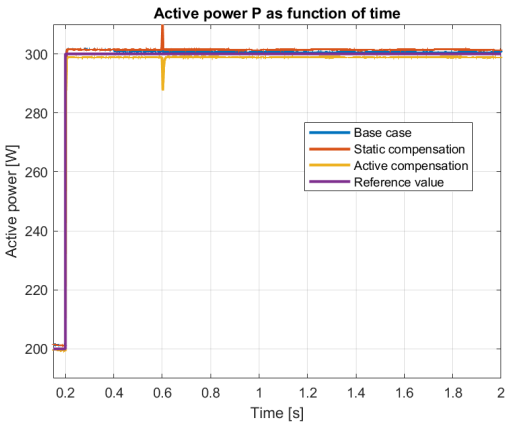

(a) Active power P for the different cases of voltage regulation.

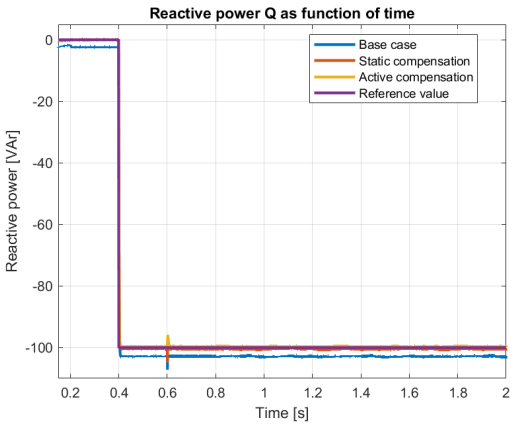

(b) Reactive power Q for the different cases of voltage regulation.

Figure 5.5: Comparison of P and Q with their reference values.

In Fig. 5.6 the phase voltages and phase currents of the inverter is shown. At 0.8 s the frequency changes from 50.0 Hz to 50.5 Hz. Measuring each phase's zero crossing, the frequency can be established to have changed in the next time period for both the voltage and current. A selection of values used to determine the response of the frequency change is shown in Fig. 5.6, however all phases in all three cases have been investigated and they show the same result. The response in frequency change is considered to have good performance.

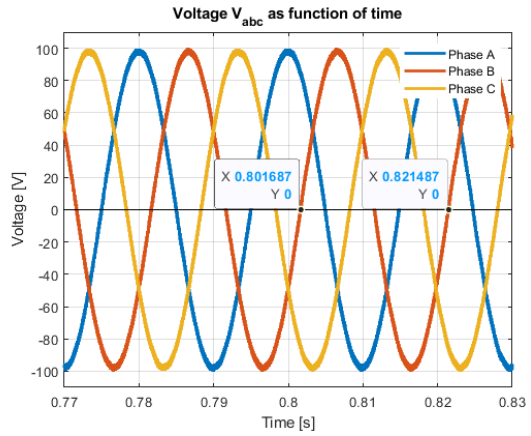

(a) Phase voltage during change of frequency.

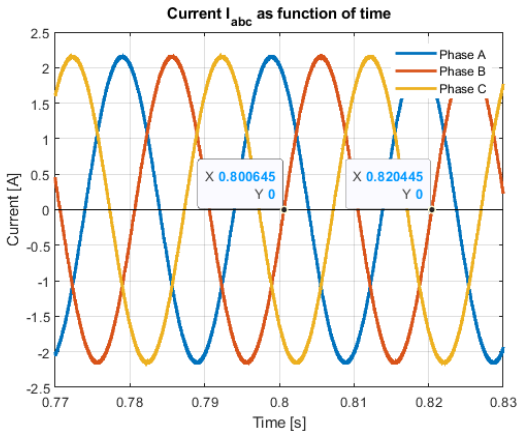

(b) Phase current during change of frequency.

Figure 5.6: Frequency change from 50.0 Hz to 50.5 Hz at 0.8 s.

The time constant (0-63%) for the system is about 1.5ms. The rise time (10-90%) is about 2.5 ms The result of the system's response can be seen in Fig. 5.7. Considering the period time is 20 ms, the 2.5 ms rise time indicates that the system is fast.

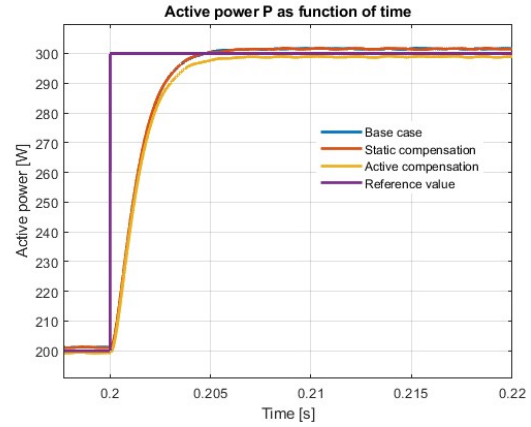

(a) The active power's response to change from 200 W to 300 W.

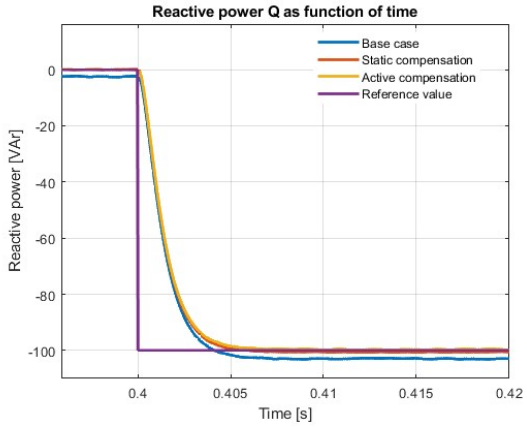

(b) The reactive power's response to change from 0 VAr to -100 VAr.

Figure 5.7: System's response to changes.

5.2 Laboratory Tests

In this section tests were conducted on the inverters to test the performance and speed if new reference values were set.

5.2.1 Voltage Regulating Tests

To test the voltage regulation and see the performance of the inverter a program was written to see what happens with sudden changes in voltage amplitude and frequency. To evaluate the performance then during change in amplitude of phase the speed of the operation was reviewed. Tests were performed in a cycle to see when the amplitude changed from the nominal value of 110V RMS to an increase to 120V and then a decrease to 100V. Then a cycle of tests with frequency changes where the frequency change from 50Hz to 49.5Hz then back to 50Hz and at last increase to 50.5Hz.

In Fig. 5.8 and Fig. 5.9 the two solutions for the voltage regulating inverters' waveform are depicted. Both solutions show good sinusoidal waveform and quick response to amplitude changes. The solution using transformers have greater amplitude variation between phases compared to the high voltage inverter solution. It is desirable to have symmetrical phases, therefore in this aspect, the high voltage inverter is superior to the transformer solution in this configuration.

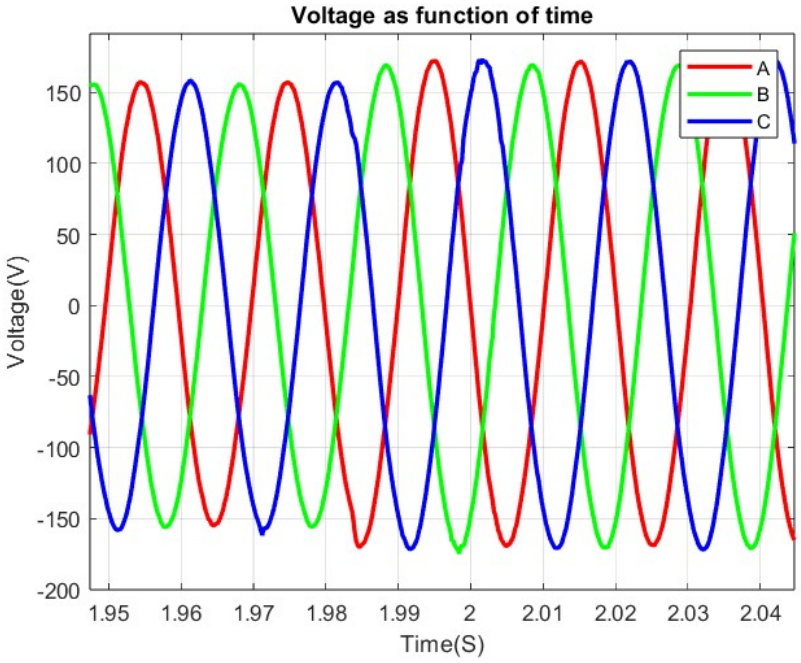

Figure 5.8: Change in amplitude for the 48 V_{DC} supplied inverter using transformers to obtain desired output voltage.

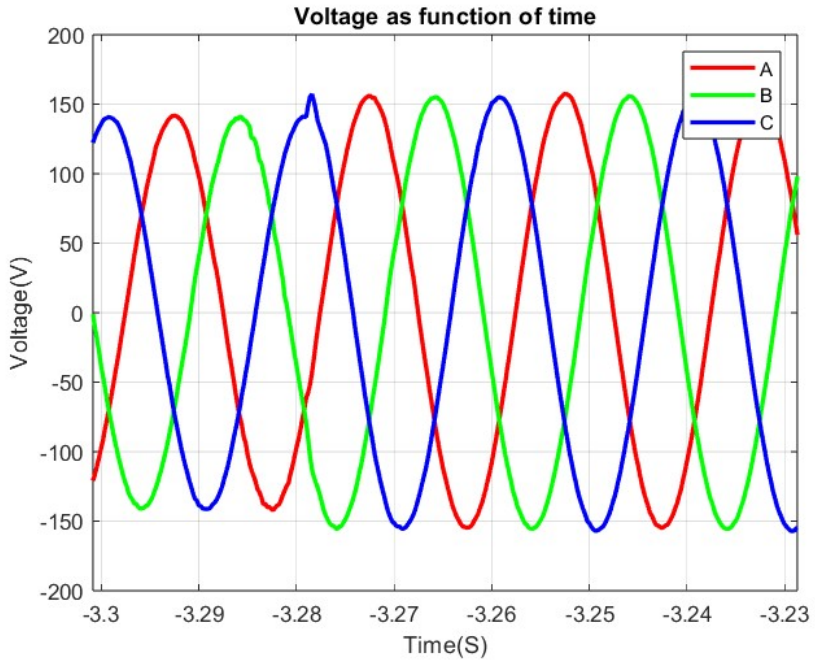

Figure 5.9: Change in amplitude for the 230 V_{rms} supplied inverter.

The rise time of the two inverter setups is similar, as can be seen in Fig. 5.10 where the blue curve represents the voltage RMS value of the solution utilizing transformers and the red curve represents the voltage RMS value of the high voltage inverter solution.

Regarding the frequency then both applications showed a smooth transition from one frequency to another when it experienced low frequency changes.

One inconsistency with comparing the two different inverter application is that for the voltage converter utilizing a lower voltage there was a bigger occurrence of voltage ripple on the wave, especially at the top and bottom of the period which distorted the sinusoidal signal to a certain degree. By calculating the RMS value for each period, it shows how big the ripple is and the deviation from the set voltage from the microprocessor. Fig. 5.10 shows the result.

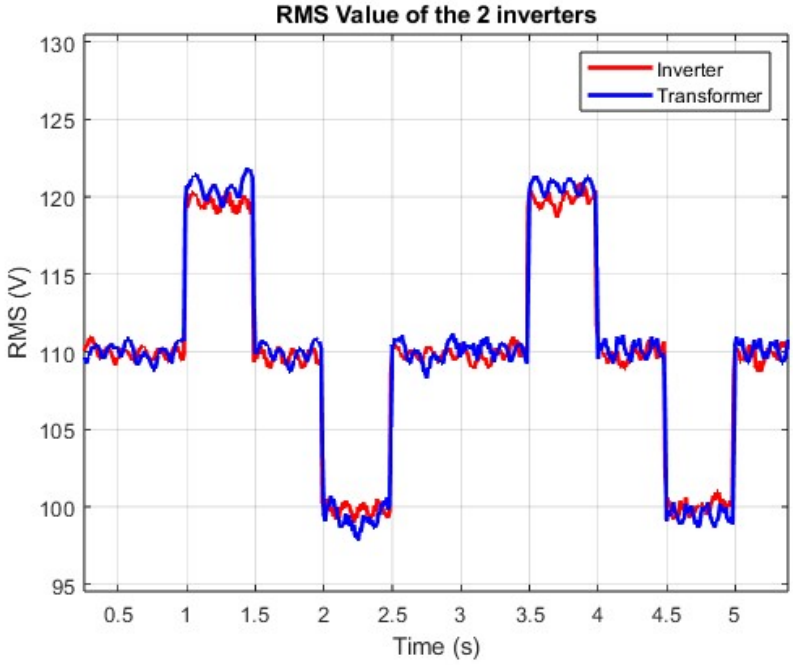

Figure 5.10: RMS of the voltage for the 2 inverter setups

The red graph named inverter shows only using the higher voltage inverter while the blue graph shows the low voltage converter coupled with transformers to raise the voltage to the set value. Here the difference in voltage ripple from the waveform is more apparent. For inverter with transformer combo when the voltage was either raised or lowered from the set value of 110V RMS then it showed a bigger ripple and deviation from the set values meaning changes in voltage amplitude will cause more ripples on the voltage while by simply using the converter the voltage stayed relatively stable with the ripples having a much less deviation from the set voltage. This probably caused by the use of transformers which add another layer of complexity to the circuit and more points of failure.

5.2.2 Current Regulating Tests

The realization of the current regulating inverter encountered problem with the feedback loop. More specifically, the signals from the current probes to the analog input of the MPU is noisy and full of disturbances. The MPU is pushed with code that shuts the inverter down if too high current is measured for protection. The noisy signals from the current probe triggers this current protection immediately. In attempts to solve the problem with noisy signals, different types of current probes were tested. In Fig. 5.11a two different probes are compared measuring the same signal. Probe 2 (see figure) is clearly less noisy and the two probes have different phase shifts. In Fig. 5.11b three phases are measured with Probe 2. From Fig. 5.11b it is evidently still a very noisy signal causing problem in the feedback loop of the inverter.

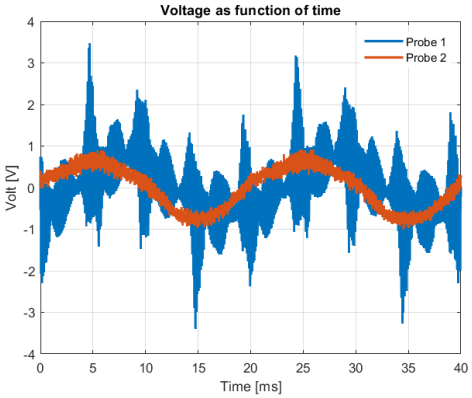

(a) Comparison between the same measurement of two different current probes.

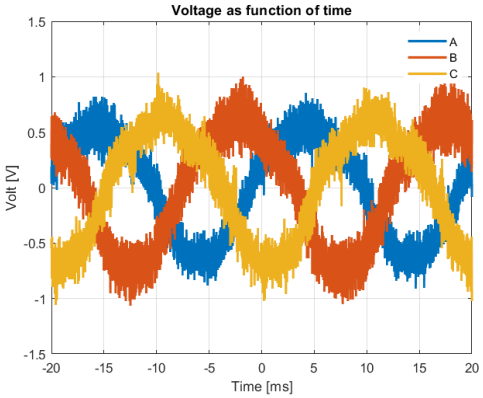

(b) Probe 2: 3-phase current measurements.

Figure 5.11: Measuring with current probes.

6
Conclusion

In this thesis, a design for test equipment for power production facilities has been developed, along with an investigation into how transducers installed in the power generating facilities impact the testing results.

In the design of the test equipment, consisting of two inverters with mutual control, simulations show promising results with output characteristics following the desired. The voltage regulating inverter was realized in two configurations, each having its respective advantages. The physical system as a whole has not yet been validated due to an incomplete current regulating converter.

The objective of this thesis was to further develop an existing testing unit to go from being solely compatible with voltage providing transducers to be compatible with the more modern/advanced transducers providing both voltage and current. Furthermore, the thesis included an investigation about what influence the inherent characteristics of the transducers have on the regulating systems. The conclusion is that the transducers overall is fast enough to make no significant impact on the regulating system.

The final product can be improved in several ways. The current measurement needs to be more accurate to effectively run the feedback control. With both the inverters up and running, the system can be evaluated and compared with the simulated results. PI-parameters may have to be tuned and voltage output can be compensated to improve the accuracy of the system.

Bibliography

[1] Svenska Kraftnät, "Information on different ancillary services." Webpage, May 2024.

[2] "Ieee code of ethics." https://www.ieee.org/about/corporate/governance/p7-8.html.

[3] MSB, "Lista med viktiga samhällsfunktioner." https://www.msb.se/sv/publikationer/identifiering-av-samhallsviktig-verksamhet–lista-med-viktiga-samhallsfunktioner/.

[4] M. Taylor, S. Al-Zoghoul, and P. Ralon, "Renewable power generation costs in 2022," *IRENA*, 2023.

[5] N. Mohan, T. M. Undeland, and W. P. Robbins, *Power Electronics: Converters, Applications, and Design*. Hoboken, NJ, USA: Wiley, 3rd ed., 2003.

[6] S. Lundberg, "Electric drive systems lecture notes." PowerPoint presentation, January 2023. Course: Electric Drive Systems (ENM076), Chalmers University of Technology.

[7] L. Harnefors, *Control of Variable-Speed Drives*. Västerås, Sweden: Applied Signal Processing and Control, Department of Electronics, Mälardalen University, 2002.

[8] K. Thorborg., *Power Electronics - in Theory and Practice.* Lund, Sweden: Studentlitteratur, 1997.

[9] N. Davis, "Safety capacitors first: Class-x and class-y capacitors," *All About Circuits*, May 2019.

[10] Svenska Kraftnät, "Testprogram för fcr-n." Webpage, November 2023.

[11] Svenska Kraftnät, "Kraftparksmodul: Bilaga 5." Webpage, April 2022.

DEPARTMENT OF SOME SUBJECT OR TECHNOLOGY
CHALMERS UNIVERSITY OF TECHNOLOGY
Gothenburg, Sweden
www.chalmers.se

CHALMERS
UNIVERSITY OF TECHNOLOGY